

**GREEN SYNTHESIS OF TiO_2 NPS USING *XIMENIA CAFFRA* LEAF
EXTRACT AND THEIR APPLICATION IN POULTRY FEEDS AS AN
ANTIBACTERIAL AGENT.**

By

MUTORITI TALENT TAWANDA

(R134170H)

Submitted in partial fulfillment of the requirements for the degree of
Bachelor of Science Honours Degree in Chemical Technology

Department of Chemical Technology

in the

Faculty of Science and Technology at the

Midlands State University

Supervisor: Mrs. N.P. Zinyama

Co-supervisor: Dr. M. Shumba

May 2017

DEDICATION

Special dedication to my grandparents, Rosemary and Dominic Chando, for their kindness, support and prayers. Not forgetting my late parents for their love, guidance, care and concern.

ACKNOWLEDGMENT

Thankful to Jesus Christ, the embodiment of wisdom who provides accurate insight into reality for his divine intervention during my research. I would like to express my deep gratitude to Mrs. N.P Zinyama and Dr M. Shumba, my supervisors, for their guidance, suggestions and encouragement on the research. My grateful thanks are also extended to Dr Chigondo, Mrs. Parerenyatwa and Mr. Mambanda for their help in maintaining my progress on schedule.

I am also grateful to my loving friends and classmates for their support. Many thanks to my family members for their financial support and encouragement (negative or positive) throughout my study.

ABSTRACT

Phytosynthesis of TiO₂ NPs from *Ximenia Caffra* leaf extract and their application in poultry feeds as an antibacterial agent was done. Reaction time and pH effect for the synthesis of TiO₂ NPs were optimized using a single factor method. A Central Composite Design (CCD) was used to determine the effect of linear factors (titanium tetrachloride concentration, temperature and leaf extract volume) and their interactions on the synthesis of TiO₂ NPs. A total of twenty experiments formulated from the central composite design were carried out, measuring absorbance as the response. Optimum conditions for the synthesis were 5 hrs, pH 7, 9 mM TiCl₄, 11 ml extract and 33 °C. UV-Vis and FT-IR techniques were used to characterize the synthesised nanoparticles. FT-IR spectra of synthesized TiO₂ NPs exhibited prominent peaks at 3440 cm⁻¹ phenol (O-H stretch), 3109.06 cm⁻¹ carboxylic acids (O-H stretch), 2108.62 cm⁻¹ alkynes and 1075.04 cm⁻¹ (C-O) (stretch alcohols, carboxylic acids, esters). An absorption peak at 400 nm confirming the presence of TiO₂ NPs was observed in the UV-visible spectrophotometric graph. Photocatalytic effect of the phytosynthesized TiO₂ NPs and feed paste were tested by disc diffusion and colony forming unit methods against pathogenic *E.coli*. The minimum zone of inhibition were observed at concentration of 5 mg/ml (TiO₂ NPs) and 11 mg/ml (TiO₂ NPs Feed paste). Green synthesized TiO₂ NPs indicates a promising approach that can satisfy their use as an antibacterial agent in poultry feeds.

DECLARATION

I, Mutoriti Talent Tawanda, hereby declare that I am the sole author of this dissertation.

I authorize Midlands State University to lend this dissertation to other institutions or individuals for the purpose of scholarly research.

Signature

Date

APPROVAL

This dissertation entitles “Green synthesis of TiO₂ NPS using *Ximenia Caffra* leaf extract and their application in poultry feeds as an antibacterial agent” by Mutoriti Talent Tawanda meets the regulations governing the award of the degree of Chemical Technology of the Midlands State University, and is approved for its contribution to knowledge and literal presentation.

Supervisor

Date

TABLE OF CONTENTS

| | |
|------------------------------|------|
| DEDICATION..... | i |
| ACKNOWLEDGMENT..... | ii |
| ABSTRACT..... | iii |
| DECLARATION..... | iv |
| APPROVAL..... | v |
| TABLE OF CONTENTS..... | vi |
| LIST OF TABLES..... | xii |
| LIST OF FIGURES..... | xiii |
| LIST OF ABBREVIATIONS..... | xiv |
| CHAPTER ONE..... | 1 |
| INTRODUCTION..... | 1 |
| 1.1 Background..... | 1 |
| 1.2 Aim..... | 3 |
| 1.3 Objectives..... | 3 |
| 1.4 Problem statement..... | 4 |
| 1.5 Justification..... | 4 |
| 1.6 Ximenia Caffra..... | 5 |
| 1.6.1 Plant description..... | 5 |
| CHAPTER TWO..... | 7 |
| LITERATURE REVIEW..... | 7 |
| 2.0 Introduction..... | 7 |

| | |
|--|----|
| 2.1 Nanoparticles | 7 |
| 2.1.0 Crystal structure of TiO ₂ | 8 |
| 2.2 Methods for synthesis of Titanium dioxide nanoparticles..... | 10 |
| 2.2.0 Chemical Method..... | 10 |
| 2.2.1 Sol–Gel Method..... | 10 |
| 2.2.2 Solvothermal..... | 10 |
| 2.2.2.1 Disadvantages of chemical methods..... | 11 |
| 2.2.3 Mechanical Grinding | 11 |
| 2.2.3.1 Demerits of mechanical | 11 |
| 2.3.0 Biosynthesis of TiO ₂ NPs methods..... | 11 |
| 2.3.1 Synthesis of TiO ₂ NPs from fungus..... | 12 |
| 2.3.1 Synthesis of TiO ₂ NPs using Yeast..... | 12 |
| 2.3.2 Synthesis of TiO ₂ NPs using Bacteria | 12 |
| 2.3.2.1 Drawbacks of using microorganisms..... | 12 |
| 2.3.3 Synthesis from Plants..... | 13 |
| 2.4.0 Phytochemical description..... | 14 |
| 2.4.1 Flavonoids..... | 14 |
| 2.4.2 Phenolic acids | 14 |
| 2.4.3 Alkaloids..... | 15 |
| 2.5.0 Application of TiO ₂ NPs..... | 16 |
| 2.5.1 Nanotechnology in Medicine..... | 16 |

| | |
|---|----|
| 2.5.2 Water purifying applications..... | 17 |
| 2.5.3 TiO ₂ NPs Antibacterial Activity | 17 |
| 2.6.0 Mechanism of Bacterial Resistance | 19 |
| 2.7 Characterization Techniques..... | 20 |
| 2.7.1 FT-IR..... | 20 |
| 2.7.2 UV.Vis | 20 |
| 2.7.2 SEM | 21 |
| 2.7.3 XRD | 21 |
| CHAPTER THREE | 23 |
| 3.0 Introduction..... | 23 |
| 3.1.Reagents..... | 23 |
| 3.1.2 Equipment/ Instrumentation..... | 23 |
| 3.2 Plant Identification and Sample collection | 24 |
| 3.3 Sample preparation | 24 |
| 3.4 Phytochemical analysis..... | 25 |
| 3.4.1 Test for phlobatannins..... | 25 |
| 3.4.2 Test for Saponins (Froth test)..... | 25 |
| 3.4.3 Test for Cardiac Glycosides | 25 |
| 3.4.4 Liebermann- Burchard Steroids Test | 25 |
| 3.4.5 Test for phenolic compounds | 25 |
| 3.4.6 Test for proteins | 26 |

| | |
|---|----|
| 3.4.7 Test for terpenoids | 26 |
| 3.4.8 Test for Quinone | 26 |
| 3.4.9 Test for flavonoids | 26 |
| 3.4.10 Test for Tannins | 26 |
| 3.4.11 Test for alkaloids..... | 26 |
| 3.4.12 Test for carbohydrates..... | 27 |
| 3.4.13 Test for Anthraquinones..... | 27 |
| 3.5.0 Nanoparticle Synthesis..... | 27 |
| 3.5.1 Optimization of pH | 27 |
| 3.5.2 Optimization of time | 27 |
| 3.6.0 Experimental Design..... | 28 |
| 3.6.1 Response Surface Methodology..... | 28 |
| 3.6.2 Synthesis of TiO ₂ NPs | 30 |
| 3.7.0 Characterisation Techniques | 31 |
| 3.7.1 Characterising using FTIR..... | 31 |
| 3.8.0 Bioactivity..... | 31 |
| 3.8.1 Identification tests | 31 |
| 3.8.2 Preparation of culture media | 31 |
| 3.8.3 Disk Preparation..... | 32 |
| 3.8.4 Culturing of bacteria | 32 |
| 3.8.5 Determination of Minimum Inhibitory Concentration (MIC) | 32 |

| | |
|---|----|
| 3.8.6 Mean Inhibition Zone..... | 32 |
| 3.8.7 Feed Paste Preparation and Bioactivity test..... | 32 |
| 3.8.8 Colony Forming Unity (C.F.U) Bioactivity test | 33 |
| CHAPTER FOUR..... | 34 |
| 4.0 Introduction..... | 34 |
| 4.1 Qualitative phytochemical analysis of X.Caffra leaf extract | 34 |
| 4.2 Optimization of process parameters..... | 35 |
| 4.2.1 Effect of pH..... | 35 |
| 4.2.2 Effect of reaction time..... | 36 |
| 4.3.0 Characterization | 37 |
| 4.3.1 UV-Vis spectra of TiO ₂ NPs | 37 |
| 4.3.2 FTIR Analysis | 38 |
| 4.4.0 Experimental Design..... | 39 |
| 4.4.1 Experimental analysis | 39 |
| 4.4.2 Method Error..... | 40 |
| 4.4.3 CCD (Central Composite Design) | 40 |
| 4.4.4 Effects of measured parameters | 45 |
| 4.4.5 Method validation | 46 |
| 4.4.6 Check for outliers..... | 47 |
| 4.4.7 Surface Response Contour Plots | 48 |
| 4.5.0 Antibacterial Test..... | 51 |

| | |
|--|----|
| 4.5.1 Disk Diffusion Method | 51 |
| 4.5.2 Colony Forming Unity | 52 |
| 4.5.3 Minimum Inhibitory Concentration | 53 |
| CHAPTER FIVE | 55 |
| CONCLUSION AND RECOMMENDATIONS | 55 |
| 5.1 Conclusion | 55 |
| 5.2 Recommendations | 56 |
| APPENDIX..... | 75 |
| List A1: Apparatus..... | 75 |
| Appendix B: Data treatment | 80 |

LIST OF TABLES

| | |
|--|----|
| Table 2: 1 Phenolic Acids | 15 |
| Table 3: 1 Experimental Domain values | 28 |
| Table 3: 2 Experimental Runs | 29 |
| Table 3:2 Cont. | 30 |
| Table 4: 1 Phytochemical Results of X.Caffra Leaf Extract..... | 34 |
| Table 4: 1 Cont..... | 35 |
| Table 4: 2 Method Error Results | 40 |
| Table 4: 3 Experimental Matrix with response measured at 400 nm..... | 41 |
| Table 4.3 Cont..... | 42 |
| Table 4: 4 Model fitting test results | 43 |
| Table 4: 5 ANOVA table for the full quadratic model. | 44 |
| Table A1: Chemical Reagents..... | 75 |
| Table A2: Instrumentation | 76 |
| Table A3: Effect of pH..... | 77 |
| Table A3: Effect of reaction time..... | 77 |
| Table A4: Method Error Results | 78 |
| Table A5: Colony Forming Unity | 78 |
| Table A6: Minimum Inhibitory Concentration | 78 |
| Table A7: Zone of inhibitions (ZOI)..... | 79 |
| Table A8: X. Caffra leaf extract Antibacterial Test..... | 79 |
| Table A9: Ashoxy 20 TM Oxytetracycline zone of inhibition | 79 |
| Table C1. Paired T-test of UV- and UV+ at 10 mg/ml..... | 81 |
| Table C2: Paired t-Test of UV+ TiO ₂ NPs (60mg/ml) and standard drug..... | 82 |
| Table C3: Paired t-Test of UV- TiO ₂ NPs (60mg/ml) and standard drug | 83 |

LIST OF FIGURES

| | |
|---|----|
| Figure 1: 1 Ximenia Caffra leaves and fruits..... | 5 |
| Figure 2: 1 Rutile phase of TiO ₂ | 8 |
| Figure 2: 2 Anatase phase of TiO ₂ | 9 |
| Figure 2: 3 Brookite phase of TiO ₂ | 9 |
| Figure 2: 4 Flavonoids glycoside..... | 15 |
| Figure 2: 5 Structure of hydroxybenzoic acid | 15 |
| Figure 2: 6 Band gap of crystalline form of TiO ₂ NPs | 18 |
| Figure 2: 7 Photochemical production of oxidative species | 18 |
| Figure 4: 1 pH Optimization..... | 36 |
| Figure 4: 2 Optimization of Time | 37 |
| Figure 4: 3 Absorption spectra of TiO ₂ NPs in the wavelength range of 300 to 700 nm..... | 38 |
| Figure 4: 4 FTIR Spectra of X. Caffra Extract and TiO ₂ NPS..... | 39 |
| Figure 4: 5 Effects of Coded Parameters | 46 |
| Figure 4: 6 (a) Normal probability plot and (b) predicted vs actual plot..... | 47 |
| Figure 4: 7 Externally Studentized Residual plot | 48 |
| Figure 4: 8 (a) Contour plot of AB (Concentration of TiCl ₄ and X.Caffra volume) | 48 |
| Figure 4: 9 Contour plots of AC (concentration of TiCl ₄ and Temperature)..... | 49 |
| Figure 4: 10 contour plot of BC (X.Caffra and Temperature)..... | 50 |
| Figure 4: 11 Colony Forming Unit | 52 |
| Figure 4: 12 Minimum Inhibitory Concentration | 54 |

LIST OF ABBREVIATIONS

| | |
|---------------------------|---|
| TiO ₂ NPS..... | Titanium dioxide nanoparticles |
| X.Caffra..... | Ximenia Caffra |
| XRD..... | X-ray Diffractometer |
| SEM..... | Scanning Electron Microscope |
| FT-IR..... | Fourier Transform Infrared Spectroscopy |
| MIC..... | Minimum Inhibitory Concentration |
| CFU..... | Colony Forming Unit |
| UV-Vis..... | Ultra Violet Visible spectroscopy |
| ZOI..... | Zone of Inhibition |
| HWFM..... | Half width at full maximum |
| BSM..... | Broiler Starter Mesh |

CHAPTER ONE

INTRODUCTION

1.1 Background

Infectious diseases are the most common killer diseases in small scale and backyard poultry production in developing countries [1]. Bacterial infectious diseases, terrorise the poultry industry especially in areas where there is limited access to medications and some of these infections are transmitted from the host into the food chain [2]. Bacterial outbreaks are being reported throughout the world, spreading via beef, chicken and poultry is the common known vector [3]. Pathogens such salmonella and E.coli are transmitted via contaminated water and feeds, infected birds remain carriers for a long time, possibly for life [4]. In poultry industry, bacterial diseases are treated using water-soluble antibiotics or anti-bacterial drugs and some of the antibiotics are used also in humans. This is reported as one of the causes of growing microbial resistance against metal ions, antibiotics and emergence of resistant strains [5]. Several methods and procedures are being developed to counter act the development of resistant strains such as drug dosages, use of ethnoveterinary medicine, good management and the use of nanoparticles [6–8].

Synthesis of metal oxide nanoparticles is a current field of material chemistry that has attracted considerable interest due to the applications of these compounds in vast fields such as in air and water purification, medicine, information technology, catalysis, energy reservoirs, and biosensors [9,10]. TiO₂ NPs have become more useful in the field of chemistry and nanomedicine as a result of their unique antibacterial and antimicrobial properties as well as their chemical stability [11,12]. TiO₂ NPs are incorporated in cosmetics whereby creams and ointments are prepared having these nanoparticles to prevent skin aging and sun burns [10].

Successful applications of TiO₂ NPs is due to their increased surface area which contributes to an increase in surface energy thereby enhancing their microbial and bacterial inhibition [13]

Several methods have been employed in the synthesis of TiO₂ NPs which include chemical and physical means with the former being the one mostly practiced industrially [14]. These methods however have demerits as they require high pressure, high temperatures, incorporates toxic chemicals and are expensive [15]

Currently the attention has been shifted towards the use of cheaper, environmentally friendly and biocompatible methods for synthesis of these TiO₂ NPs [11]. Phytosynthesis of TiO₂ NPs has been done making use of different biological organisms such as actinomycetes, fungi, plants and bacteria [9,10,16–19] . Among the various biosynthetic proposed, the use of plant extracts has several advantages such as easy availability, safe to handle and possess a broad viability of secondary metabolites [9]. The main phytochemicals which are responsible for the oxidation/ reduction during synthesis of nanoparticles are flavones, terpenoids, coumarins, phenols, amides [9,11,13]. TiO₂ NPs have demonstrated significant antibacterial and antioxidant activity, its action is by oxidative damage to the bacteria cell wall [13].

In pursuing the efforts for synthesizing TiO₂ NPs, here we report a green synthesis using the leaf extract of *X.Caffra*. The plant has been chosen because of its antioxidant and exhibit low antimicrobial activities with recorded maximum zone of inhibition being $2.79 \pm 0.96 \text{ mm}$ [20]. The phytosynthetic route for nanoparticles has not yet been exploited for the synthesis of TiO₂ NPs using *X.Caffra*.

1.2 Aim

To synthesise TiO₂ nanoparticles using Ximenia Caffra leaf extract and its application in poultry feeds as an antibacterial agent.

1.3 Objectives

- To synthesise TiO₂ NPs using Ximenia Caffra leaf extract.
- To characterise synthesised TiO₂ NPs using UV-Vis and FTIR.
- To assess the antibacterial activity of TiO₂ NPs, plant extract and prepared feed.
- To determine the minimum inhibitory concentration of the synthesised TiO₂ NPs and the prepared feed.

1.4 Problem statement

Most rural households in Africa and other continents keep poultry native to their areas, especially chickens. The major challenge in the poultry production under rural settings include diseases, poor nutrition and predation [1]. Farmers indicate high production costs, (antibiotics, vaccines, conditioners) and stock feed shortages as other predicaments that causes high mortality in small scale poultry industry [21]. Due to the current economic situation in developing countries, it is expensive to acquire poultry medication and as a result the industry is prone to bacterial disease and pathogens transmittance through contaminated feeds and drinking water which resulting in severe economic losses [22,23]. There is need of better and cheaper biocides compatible with feed which undergoes self sanitisation and at the same time inhibiting the growth of bacteria in order to prevent and control out-break of feed and water borne bacterial infectious diseases.

1.5 Justification

Agriculture is the backbone of the Zimbabwean economy which contributes enormously to the country's gross domestic product [5]. Due to a number of reasons, urban and peri-agriculture is on the rise where there is increase in the growing of plants and raising of animals within and around cities [5]. Poultry and Pig farming are easy entry for many urban growers in Zimbabwe as indicated by the Zimbabwe Poultry Association [ZPA] that a growth of 22 percent was observed in the first quarter of 2015 after producing 17 million broiler day old chicks. Several challenges are emerging in this sector which includes a growing demand for healthy, an increasing risk of disease and threats to agricultural production from changing weather patterns [24]. Access to quality agricultural medication to support poultry farming is critical for the viability of this sector. Modern technologies can be utilised to assist urban and rural poultry farmers with medication [25]. *Escherichia coli*, *Salmonella* species, and *Staphylococcus* species are the major bacterial pathogens terrorising poultry industry in developing countries

[26]. Difference in susceptibility to antibiotics by microorganisms has become a major factor in drug choice and success of treatment [26,27]. Great concerns has been raised regarding the emergence of antimicrobial resistance among bacteria which results in antimicrobial unpredictable susceptibility and failure of therapy [26].

TiO₂ NPs have been found to be useful in treating bacterial infections thus phytosynthesis of these nanoparticles will help in dealing with bacterial infections which have become a menace due to their resistance to available medications [11,13,16,26]. Phytosynthetic methods of TiO₂ NPs are of great advantage as it eliminates the risk posed by toxic chemicals since the method does not involve the use of these chemicals [9,13,17,18].

1.6 Ximenia Caffra



Figure 1: 1 Ximenia Caffra leaves and fruits

Common name: Munhengeni

Family: Olacaceae

1.6.1 Plant description

Ximenia Caffra is a deciduous tree which attains an average height of six meters and some spikes are found on the stem of the old plants. Barks are dim and unpleasant, however light green or cocoa on the more youthful branches [20]. Branches and twigs are armed with stout axillary spines and are glabrous, regularly bristly when youthful and changes to gleaming green

while getting more seasoned and shift in size [28]. Sapwood is white and heartwood is hard and rosy chestnut [20]. The root framework is non aggressive and the blooms are little, sweet scented and rich green [20]. The tree is dispersed widely in forests and fields and on rough outcrops and in certain cases on termites hills [20,29].

TiO₂ NPs generate strong oxidizing species when illuminated with UV light with wavelengths of 400 nm. Holes (h⁺) and hydroxyl radicals (OH[·]) are produced in the valence band, and electrons and superoxide ions (O₂⁻) in the conduction band [30]. Death of microorganism is proposed to occur as a result of direct oxidation of an intracellular coenzyme A that is responsible for cell respiration [31].

There is, however lack of knowledge on the antimicrobial activity of green synthesised TiO₂ NPs from *X. Caffra* leaf extract. Thus, it is essential to research on the antimicrobial ability of these green synthesised TiO₂ NPs to establish baseline data that is essential for formulating ways of supplementing poultry medication to improve poultry farming, human health and increase profitability of the entrepreneurs thus enhancing income generation.

CHAPTER TWO

LITERATURE REVIEW

2.0 Introduction

This chapter gives an outline on nanoparticles in general and also more specifically the TiO₂ NPs. Applications of the nanoparticles are highlighted together with the various methods and analytical techniques that have been used for the synthesis of TiO₂ NPs.

2.1 Nanoparticles

Nanotechnology is a rapidly growing field with vast applications in science and technology for the purpose of developing new materials at nanoscale level [17]. Nanoparticles are solid particles of size between atoms or molecules and macroscopic objects [32]. They constitute several of tens or hundreds of atoms or molecules which vary in sizes and morphologies [33]. Nanoparticles are demonstrating special physical properties and are being widely used in variety of applications [32]. Different kinds of nanoparticles are being produced commercially in the form of dry powders or liquid dispersions. The latter is as a result of combining nanoparticles with an aqueous or organic liquid to form a suspension or paste [32]. Nanoparticles exhibit completely improved physio-chemical properties based on specific characteristics such as size, distribution and morphology [10,17]. Nanomaterials significantly affect areas of physics, chemical science, electronics, optics, materials science and biomedical science [33]. Mass production of nanoparticulate materials such as carbon black, polymer dispersions, or micronized drugs within industries has been established. One of the most important class of nanoparticulate materials is metal oxide nanoparticles that considers silica (SiO₂), titania (TiO₂), alumina (Al₂O₃) etc.

Due to the abundance of titanium dioxide, TiO₂ NPs has become a new generation of advanced materials and one of the most widely used nanostructures in various fields [34]. Titanium

dioxide is a semiconductor with a wide band gap having crystalline forms which are anatase, rutile or brookite [35]. Due to its opacity, it has been used in bulk form over the years as a white pigment in paints and in paper making process [36]. The polymorphs of TiO_2 is found to be in an octahedral coordination, i.e., having a coordination number equals six [36]. The octahedral in rutile, anatase and brookite vary with respect to their spacing relative to each other and only rutile and anatase differs from each other in their physical properties. The value of shared edges increases from two in rutile, to three in brookite, to four in anatase [35]. Rutile is thermodynamically the most stable since the relative stability in the bulk phase inversely related to the number of shared edges [36,37]. Among the three forms, anatase and brookite rearrange monotropically to rutile when exposed to elevated temperatures ranges of 750 °C to 1000 °C.

2.1.0 Crystal structure of TiO_2

Rutile: it consist of hexagonal closely packed oxygen atoms where the other half of the octahedral spaces are filled with titanium atoms.

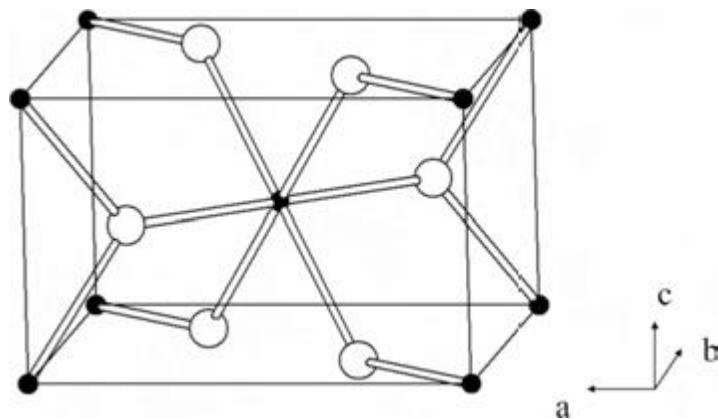


Figure 2: 1 Rutile phase of TiO_2

Black spheres: titanium atoms and white spheres: oxygen atoms

In anatase: oxygen atoms are closely packed in a cubic form having half of the tetrahedral spaces occupied by titanium atoms.

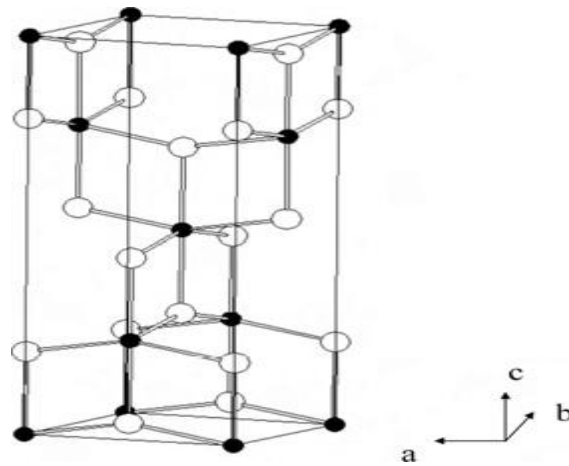


Figure 2: 2 Anatase phase of TiO_2

Black spheres: titanium atoms and white spheres: oxygen atoms

Brookite:

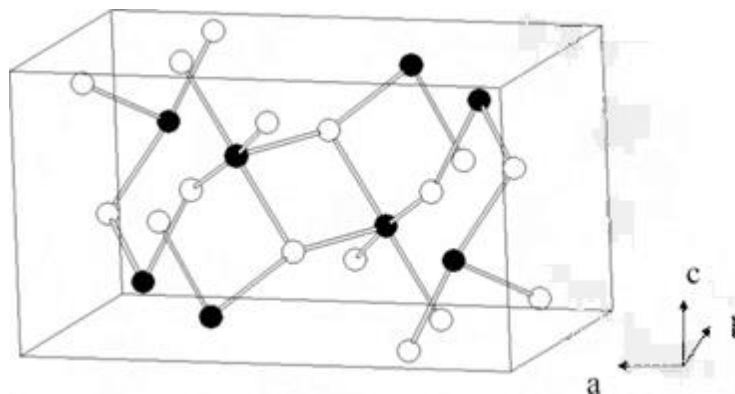


Figure 2: 3 Brookite phase of TiO_2

Black spheres: titanium atoms; white spheres: oxygen atoms

Technology has shifted attention from the bulk titanium dioxide to nanoparticles and there are several methods developed for the synthesis of these nanoparticles [36].

2.2 Methods for synthesis of Titanium dioxide nanoparticles

Synthesis of nanoparticles, one of the major objective that is important in materials science and engineering branches [38]. TiO₂ NPs are being produced by a number of chemical, physical, or biological processes, some of which are totally new and innovative, while others are of age.

2.2.0 Chemical Method

2.2.1 Sol–Gel Method

The sol–gel process involves the development of networks through the organisation of a colloidal suspension (sol) and gelation of the sol to form a network in a continuous liquid phase (gel) [39]. The process constitutes of several stages, first stage involves the synthesis of the colloid. Sol–gel processes are well adapted for metal oxide nanoparticles, starting material is processed to form dispersible oxides, titanates and forms a sol that is in contact with water or dilute acid [40]. Liquid is then removed from the sol after reaction to form a gel, the sol–gel transition controls the particle size and shape of the TiO₂ NPs. The gel takes an average of 7 days to mature and then calcination of the gel occurs to produce TiO₂ NPs [41] .

2.2.2 Solvothermal

Solvothermal reaction process is done in a stainless steel pressure vessel [42]. The synthesis method allows for the precise control over the size, shape distribution and crystallinity of TiO₂ NPs. In a typical synthesis, titanium (IV) alkoxide is dissolved in a test tube containing alcohol, which is then subjected to heat in an autoclave [42]. The autoclave is thoroughly purged with nitrogen gas, heated to desired temperature range usually (523–573 K) at a specific rate, and kept at that temperature for a required time [32]. Having done the autoclave treatment, resulting TiO₂ NPs are repeatedly washed with acetone and then air dried.

2.2.2.1 Disadvantages of chemical methods

- Makes use of vast number of chemicals which are highly toxic and hazardous
- Usually high temperature and pressure conditions are employed
- Involvement of difficult separation techniques
- Cost of running the process are expensive

2.2.3 Mechanical Grinding

Physical grinding method are being used for the size reduction of TiO₂ bulk powder. A known amount of TiO₂ bulk powder is placed in a grinding machine which has a high speed rotator [43]. TiO₂ bulk powders are subjected to grinding under a protective atmosphere to avoid contamination in equipment that is capable of high-energy compressive impact forces such as attrition [32]. The machine will uniformly grind, crush the TiO₂ bulk powder and at the end separate the finely ground powder [44]. Thus, the bulk TiO₂ powder will be having nano-sized powder [45].

2.2.3.1 Demerits of mechanical

- Expensive as special instruments are requires which withstand pressure that builds up during the process and avoiding contamination
- High energy intensive process
- Time consuming process

2.3.0 Biosynthesis of TiO₂ NPs methods

Biosynthesis involves the use of environmentally friendly green chemistry based approach that utilises unicellular and multicellular biological entities for example actinomycetes, bacteria, fungus, plants, viruses, and yeast [46]. Synthesising nanoparticles through natural sources going about as organic manufacturing plants offers a perfect, nontoxic and environment-

accommodating technique for integrating nanoparticles with a wide scope of sizes, shapes, organizations, and physicochemical properties

2.3.1 Synthesis of TiO₂ NPs from fungus

TiO₂ NPs synthesis from fungi has been done whereby the fungi are first isolated from the roots and stems of wilted tomato plants [47]. The isolated fungi are treated with borax and mercury chloride solutions [47]. Sterilized inoculums obtained are then cultured to produce a fungal hyphae which is reacted with precursor salt of titanium to produce TiO₂ NPs [19,21].

2.3.1 Synthesis of TiO₂ NPs using Yeast

Biosynthesis of TiO₂ NPs from baker's yeast was done whereby a culture solution of yeast cells was prepared using glucose aqueous solution at room temperature [38]. The mixture was stirred to produce a uniform bio-emulsion which was then reacted with TiCl₄ and hydrochloric acid (HCl) [49]. TiO₂ NPs were observed as white precipitate after 24 hours of continuous stirring [48]. The synthesis procedure was also repeated varying the precursor solutions using solution of TiO·(OH)₂ and bulk TiO₂.

2.3.2 Synthesis of TiO₂NPs using Bacteria

The method involves isolation and then culturing the selected microorganism for example *Planomicrobium sp*, *Chromohalobacter salexigens* were used for the synthesis of TiO₂ NPS [15,50]. The bacteria were cultured for 24 hours, a solution containing precursor of titanium was added and heated to a specified temperature using a water bath to form white colour depositions. The solution was allowed to cool and the nanoparticles were obtained either by direct filtration, centrifugation or decantation [51].

2.3.2.1 Drawbacks of using microorganisms

- Culturing micro-organisms is a must which may take weeks up to a month and it is not always a success [9,15,52].

- During synthesis there is need for maintaining micro-organism cell walls that makes the process laborious and time consuming [47].
- Low yields [51]

2.3.3 Synthesis from Plants

Plants are one of the important candidates which have the potential to hyper-accumulate and biologically reduce metallic ions [53]. Plants are considered to be more environmental friendly source for bio-synthesis of metallic nanoparticles and for detoxification applications [54]. Plants contain the secondary metabolites (phytochemicals) which are responsible for the defence mechanism against external threats and allow them to adapt to the changes that occur due climate changes [54]. Variations of phytochemical composition and concentration between different plants and their subsequent interaction with aqueous metal ions contributes to the formation of nanoparticles of different sizes and shapes. Bio-synthesis of nanoparticles from reducing metal salts via plants is simple and straightforward usually done at room temperature [55]. Phytosynthesis involves mixing a sample of plant extract with a precursor solution. The initial step during biochemical reduction involves activation period when metal ions are converted from their mono or divalent oxidation states to zero-valent states followed by nucleation of the reduced metal atoms [56]. As soon as the nucleation process begins, growth occurs whereby smaller neighbouring particles unify to form bigger nanoparticles which are thermodynamically stable [56]. As growth continues a variety of morphologies such as spheres, triangles, pentagons, rods, and wires are produced [23]. In the final stage of synthesis, the plant extracts ability to stabilize the nanoparticle ultimately determines it's most energetically favourable and stable morphology [55]. Phytochemicals which are responsible for the biochemical reduction of metal salts and stabilises the nanoparticles are as follows alkaloids, phenolic acids, flavonoids, proteins, sugars, and terpenoids [55].

2.4.0 Phytochemical description

2.4.1 Flavonoids

These are water soluble polyphenolic molecules having 15 carbon atoms which can be pictured with two benzene rings that are joined together with a short three carbon chain [20]. Among the three short carbon chains, one of the carbons of the short chain is always connected to a carbon of one of the benzene rings, either directly or through an oxygen bridge to form a middle ring [57]. Flavonoids pharmacological properties includes anticancer, antimicrobial, anti-inflammatory, antioxidant and antimalarial activity [58].

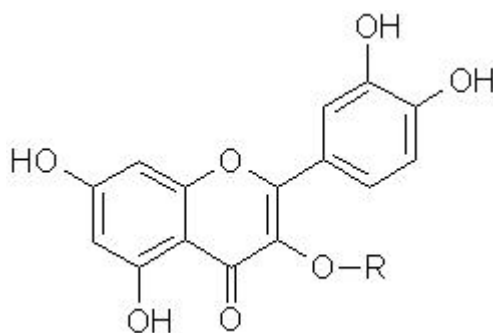


Figure 2: 4 Flavonoids glycoside

2.4.2 Phenolic acids

Phenolic phytochemicals represent the largest category of phytochemicals widespread in various fruits and vegetables and one of the major groups of secondary metabolites in plants [59]. They are divided into two classes which are derivatives of benzoic acid such as gallic acid and derivatives of cinnamic acid such as caffeic [60]. They are characterized by hydroxylated aromatic rings and possess a single carboxylic acid functional group [61]. Pharmacological properties includes anti-oxidants, anti-tumor and antibacterial activities [62].

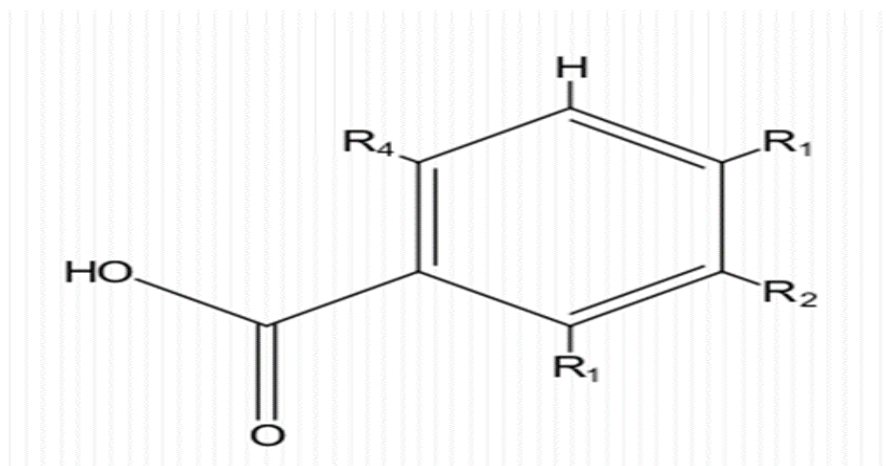


Figure 2: 5 Structure of hydroxybenzoic acid [63]

Table 2: 1 Phenolic Acids

| Position | R ₁ | R ₂ | R ₃ | R ₄ |
|----------------|----------------|------------------|----------------|----------------|
| Benzoic acid | H | H | H | H |
| Gallic acid | H | OH | OH | OH |
| Vaillinic acid | H | OCH ₃ | OH | H |
| Salicylic acid | OH | H | H | H |

2.4.3 Alkaloids

Alkaloids are basic substances that contain one or more nitrogen atoms, usually in combination or as part of a cyclic system [64]. Alkaloids contains a complex molecule structure and having significant pharmacological activities [32].The nitrogen generally makes the compound basic and the compound are found in the plant as a salt .

TiO₂ NPs synthesis from plant extracts is of current interest due to the availability of different phytochemicals which are found within the kingdom plantae that stabilises nanoparticles. *Aloe vera*, *Nyctanthes arbor-tristis*, *Curcuma longa*, *Psidium guajava* and *Moringa oleifera* are some the plants that were reported to have been used for the synthesis of TiO₂ NPs

[9,11,13,16,18]. For example, *Annona squamosa* peel reportedly used to effectively synthesize TiO₂ NPs, while *Nyctanthes arbor-tristis* leaf extract yields spherical particles of size that ranges from 100 to 150 nm [257] and *Eclipta prostrata* leaf extract produces particle sizes of 36 to 68 nm [9,65]. The use of *Catharanthus roseus* leaf extract for phytosynthesis of TiO₂ NPs reported to produce nanoparticles with irregular shape that ranges from 25 to 110 nm [66].

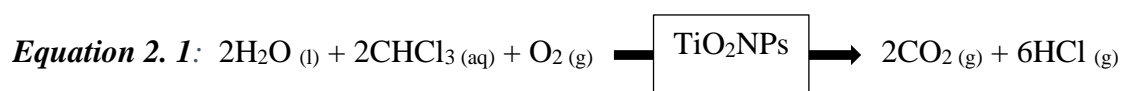
2.5.0 Application of TiO₂ NPs

2.5.1 Nanotechnology in Medicine

Nanomedicine includes utilization of nanotechnology for the benefit of ethnical health and well beings [67]. Biomedical nanotechnology affords progressive possibilities among the fight towards many disease causing pathogens [68]. Nanotechnology provides extraordinary ways that improves materials and medical devices and also creates unique devices with better performance than the existing conventional technology [69]. Advanced drug delivery system are being developed which aims to enhance bioavailability and pharmacokinetics of pharmaceuticals and to substitute invasive administration methods [70]. Nano-carriers which consist of optimized physicochemical and biological properties are more easily taken up by cells than larger molecules and it acts as a successful delivery tools for currently available bioactive compounds [71]. The delivery systems is site-specific which targets a specific cell or tissue [72]. TiO₂ NPs reported to be a promising candidate that acts against malignant brain tumors which are resistant to conventional therapies [73]. TiO₂ NPs linked to an antibody are used to recognize, bind specifically to cancer cells and a beam of visible light is focused onto the affected region to induce photo-killing of the cancer cells by free radical mechanism [74,75]. TiO₂ NPs are reported to be used in wound healing, antibacterial, antifungal, antioxidants and some as antiviral activities [76–78].

2.5.2 Water purifying applications

It has been reported that TiO₂ NPs induces detrimental organic substances such as organic chlorine compounds and other toxic substances to disintegrate into less harmful products [79]. In water purification given for example chloroform in the presence of TiO₂ NPs, it will break down as illustrated by the equation below:



2.5.3 TiO₂ NPs Antibacterial Activity

There is an increase in the number of microbial resistance against antibiotics, metal ions and also the development of new resistant strains [80]. TiO₂ NPs are of current interest as they have demonstrated significant antibacterial activity [81]. Titania nanorods synthesized by sol-gel electrospinning technique has been reported to have an antibacterial activity when tested against *S. aureus*, *E. coli*, *Klebsiella pneumonia* and *Salmonella typhimurium* [82]. Evidence deduced experimentally has shown that exposure to TiO₂ NPs and UV radiation destroys cells by generating oxidative stress [83]. Oxidative stress is reported to be an emerging fundamental mechanism of nanoparticles toxicity [84]. Bacteria cell wall is reported to be damaged by oxidation process which leads to a decrease in the interfacial energy of bacteria adhesion causing an increase in the chemical interaction between bacteria and the nanoparticles, an additional factor for increasing bactericidal activity [85]. When TiO₂ NPs photo-irradiated with UV light suitable to their bandgap energy of 3.06 eV (rutile), 3.2 eV (anatase), or higher, they have a propensity to experience all physical phenomena which involves absorption, reflection and scattering of light [86]. Other essential process also occurs which involves photophysical and photochemical processes. During photophysical process, the absorbed photons of light result in the excitation of electrons (e⁻) from the valence band to the conduction band creating holes (h⁺) in the valence band which generates electron and hole pairs [87]. Energized electron

and hole pairs are said to either recombine and release energy as heat or dissociate because of charge trapping thus producing charge carriers resulting in the redox reaction of materials adsorbing on the surface such as water and molecular oxygen [88]. UV light on the surface of TiO₂ NPs stimulates the formation of various reactive species when reacted with water or oxygen that leads to the damage of bio-macromolecules [89]. Reactive species formed by photo-irradiating are h⁺, hydroxyl radicals (OH[•]), superoxide (O₂^{•-}), hydrogen peroxide (H₂O₂), and singlet oxygen (¹O₂) [90]. Photocatalyzed formation of singlet oxygen was suggested that it contributes to the oxidation of the protein membranes [91]. Hydroxyl radicals plays the most crucial role in deactivating microorganism by oxidizing the polymers of unsaturated phospholipid that makes up the microbial cell membrane.

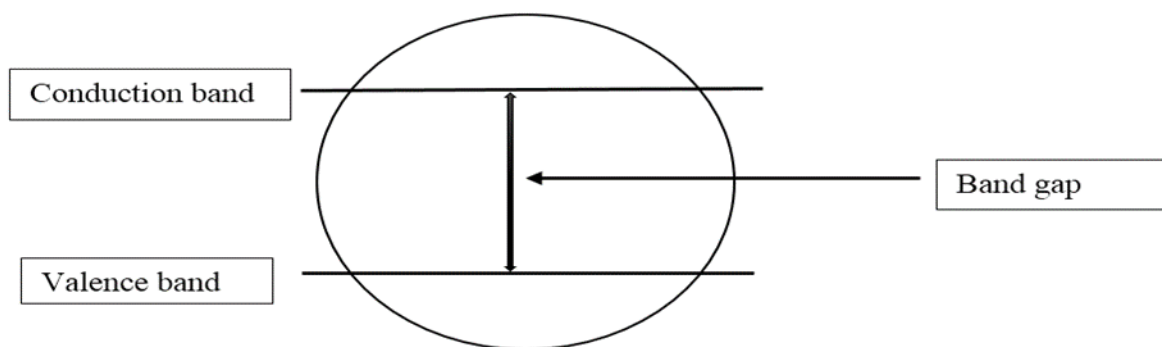


Figure 2: 6 Band gap of crystalline form of TiO₂ NPs

Photochemical Reaction Process

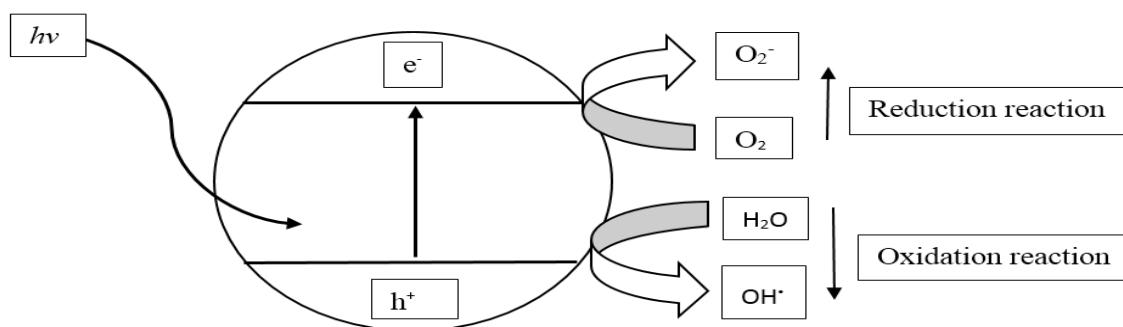
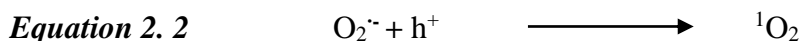


Figure 2: 7 Photochemical production of oxidative species

Photocatalytic formation of reactive oxygen species

The singlet oxygen is formed when O_2^- produced by TiO_2 NPs photocatalysis is reoxidised on the h^+ of TiO_2 NPs surface. Equation for the reaction to produce singlet oxygen is as follows:



2.6.0 Mechanism of Bacterial Resistance

Bacterial resistance occurs as result of either natural or acquired mechanism. Natural resistance results when the properties of a bacteria inhibits the action of a certain antibiotic [92]. As reported, an antibiotic designed to attach to certain specific receptors on a bacterial cell is unable to act if the bacterial species does not have the receptors. Acquired resistance results due to alteration of bacterial species and its genetic makeup in such a manner that it decreases the action of antibiotics [93]. There are several ways in which the bacterial genome can be altered such as vertical gene transfer, horizontal gene transfer. Vertical gene transfer is whereby random mutations and reproduction confer resistance on the next generations while horizontal gene transfer involves genetic information being conferred to members of the exact generation [94].

In both vertical and horizontal gene transfer bacterial genetic characteristics are varied, altering their own physiology, qualifying them to respond to environmental factors like antibiotics [94]. Physiological alterations consist of four major mechanisms which are drug inactivation (modification), target site alteration, making use of different metabolic pathways and reduction of drug accumulation within cell [95].

2.7 Characterization Techniques

2.7.1 FT-IR

Infrared spectroscopy is a non-destructive technique for materials analysis and it is used to study the interaction between an infrared radiation with a sample that can be solid, liquid or gaseous as a function of photon frequency [96]. FT-IR provides exact information concerning the vibration and rotation of the chemical bonding and molecular structures [97]. An infrared spectrum obtained during analysis represents a fingerprint of a sample with absorption peaks which correspond to the vibrational frequencies between atomic bonds making up the sample [98]. Vibrational transitions which occurs as a result of infrared photon correspond to distinct energies, and molecules absorb infrared radiation only at certain wavelengths and frequencies [99]. These frequencies are helpful for the identification of the sample's chemical make-up since no two compounds produce the exact same infrared spectrum [99].

2.7.2 UV.Vis

UV spectroscopy is a technique of absorption spectroscopy whereby light in the ultra-violet region is absorbed by the molecule. The absorbed electromagnetic radiations will result in changes in electronic structure of ions and molecules through the excitations of bonded and non-bonded electrons [100] . The energy absorbed is equal to the energy difference between the ground state and higher energy states. The technique is useful for quantification of light which a sample absorbs with respect to the wavelength of radiation [101] .The technique obeys the Beer-Lambert law, which states that there is a linear relationship between the absorbance and the concentration of a sample [102,103] . Thus:

$$\text{Absorbance } A = \text{constant} \times \text{concentration} \times \text{cell length}$$

By making use of the Beer-Lambert law, it has been found that the greater the number of molecules capable of absorbing light of a given wavelength, the greater the extent of light absorption [103,104].

2.7.2 SEM

The scanning electron microscope is used for the examination and analysis of the microstructure morphology and chemical composition characterizations [13]. An electron beam is focused onto the sample surface kept in a vacuum by electro-magnetic lenses and the beam is then scanned over the surface of the sample [105]. Scattered electrons from the sample are fed to the detector and then to a cathode ray tube through an amplifier, where images are formed, portraying information on the sample surface [106].

2.7.3 XRD

The XRD pattern of a pure substance is used as a fingerprint of that particular substance. One of the main application of XRD is to identify components within a sample by a search and match procedure [107]. Crystalline substances behave as 3D diffraction gratings for X-ray wavelengths similar to the spacing of planes in a crystal lattice. XRD is derived from constructive interference of monochromatic X-rays and the crystalline sample. Cathode ray tube generates x-rays which are filtered to produce a monochromatic radiation, adjusted to concentrate, and directed toward the sample under analysis. The interaction between the incident rays and the sample produces constructive interference and a diffracted ray when conditions are in sync with the Bragg's Law. The law is satisfied by an equation; $n\lambda = 2d \sin \theta$ which relates the wavelength of electromagnetic radiation to the diffraction angle and the lattice spacing within the crystalline sample. Diffracted X-rays are detected, processed and then counted [107]. The sample is scanned through a range of 2θ angles so that all possible diffraction directions of the lattice can be attained because of the random orientation of the

powdered sample. Identification of the sample is done by conversion of the diffraction peaks to d-spacings, compares it with standard reference patterns because each sample has a set of unique d-spacings [108]. Particle size can be calculated from the peak area as width of peaks of a given pattern provides information on the crystalline's average size. The larger the crystallite the sharper are the peaks. The Scherrer equation is used to calculate the crystallite particle size and it is given as follows:

$$D = \frac{k\lambda}{\beta \cos \theta} \quad \text{Whereby } \beta = \text{HWFM} \times \frac{22}{7 \times 180}$$

θ is the Bragg angle,

λ (the X- ray wavelength used),

β is the width (full) at half the maximum diffraction peak in the 2θ scale in radians

k Scherrer constant with a value of 0.9

HWFM is the half width at full maximum for the diffraction peak with maximum intensity.

CHAPTER THREE

METHODOLOGY

3.0 Introduction

The chapter focuses on the experimental procedures that were carried out to achieve the aim and objectives in this research.

3.1.1 Reagents

All chemicals utilized for vast experiments in this research were of analytical reagent grade unless otherwise stated and were utilized without undergoing additional purification process. Distilled water was used in every part of the research for different purposes. The most important reagents used were aqueous titanium tetrachloride (TiCl_4 , 16-17 % wt.) , Acetic anhydride ($(\text{CH}_3\text{CO})_2\text{O}$ 40 %), ferric chloride (FeCl_3 , 5 % w/v), sodium hydroxide (NaOH, 10%), sulphuric acid (H_2SO_4 , 98 %), potassium iodide (KI, 99.9 %), Chloroform (CHCl_3 , 55 %), potassium bromide (KBr, 99.9 % FT-IR grade), glacial acetic acid (CH_3COOH , 99.7 %) , hydrochloric acid (HCl, 30%), dichloromethane (CH_2Cl_2 , 99.8 %), ammonia (NH_3 , 10 %) , Copper sulphate (CuSO_4 , 1%) and methanol (CH_3OH , 75 %).

3.1.2 Equipment/ Instrumentation

- ❖ Laboratory incubator model LABOTEC M15 was used to provide a controlled, contaminant-free environment for safe, reliable work with bacterial cultures by regulating temperature, humidity, and CO_2 . The incubator was used mainly to optimize the growth of pathogenic bacterial E.coli.
- ❖ Autoclave RAU-123 was used to sterilize laboratory equipment which were used for culturing the bacterial E.coli and also the nutrient agar.
- ❖ Vortex Shaker QL 866 was used for deglomeration of nanoparticles and allow an even distribution of particles within a prepared mixture.

- ❖ Laboratory analytical balance model JJ 224 BC was used for weighing all the samples used in this research, from reagent to products formed.
- ❖ Water bath ZWY 110X30 was used for controlling the heating temperature during the synthesis of titanium dioxide nanoparticles.
- ❖ UV-Vis 752 model was used to measure the absorbance of the synthesized titanium dioxide nanoparticles during optimization reaction and also to characterize the synthesized nanoparticles.
- ❖ FTIR Nicolet 6700 instrument was used in the determination of functional groups associated with extract and that of the synthesized titanium dioxide nanoparticles.

3.2 Plant Identification and Sample collection

Plant identification was done with the help of a qualified botanist. Fresh leaves of *X. Caffra* were randomly collected from more than four different plants in Mkoba Village. The leaves were placed in a polyethylene plastic bag and transferred to the laboratory on the same day.

3.3 Sample preparation

The collected *X. Caffra* leaves were washed with running tap water followed by distilled water to remove the unwanted impurities such as scum, dust and other particulates [109]. The leaves were dried at room temperature. After complete drying when a constant mass was attained, leaves were ground into powder and sieved to achieve a homogeneous particle size of 2 mm in diameter. A mass of 25.0020 g dried leaves were suspended in 100 ml distilled water subjected to shaking on a rotary shaker for 24 hours under room temperature and the mixture was filtered by suction method, the extract produced was stored in a refrigerator [15].

3.4 Phytochemical analysis

The solution of 10 ml extract was obtained from the refrigerated volumetric flask and heated using a hot plate up to a temperature of 30°C and was allowed to cool to a room temperature for analysis.

3.4.1 Test for phlobatannins

A volume of 5 ml dilute hydrochloric acid (1%) was added to 2 ml of plant extract followed by boiling on a hot plate with a stirrer. Positive test of phlobatannins is indicated by the formation of a red coloured precipitate [110].

3.4.2 Test for Saponins (Froth test)

Saponins were tested by dissolving 1 ml of the sample extract in a test tube containing 6 ml of hot distilled water. The mixture was subjected to vigorous shaking for approximately one minute and persistent foaming indicates the positive [111,112].

3.4.3 Test for Cardiac Glycosides

To a 1 ml of extract, 1 ml of glacial acetic acid containing a drop of ferric chloride solution was added followed by 1 ml of concentrated sulphuric acid. A positive result is indicated by formation of a reddish brown colour [113].

3.4.4 Liebermann- Burchard Steroids Test

A volume of 5 ml of extract was added to 10 ml dichloromethane followed by addition of 10 ml of acetic anhydride. Drops of concentrated sulphuric acid were added while observing any colour changes and appearance of greenish blue colour indicates the presence of steroids [114].

3.4.5 Test for phenolic compounds

From the stock, 1 ml of extract was obtained and three drops of 5 % FeCl₃ (w/v) were added. A positive result is indicated by formation of a greenish precipitate [57].

3.4.6 Test for proteins

A volume of 1 ml (4 %) solution of NaOH and 1 ml (1 %) CuSO₄ were added to 1 ml of leaf extract. Appearance of a pink or purple colour indicates the presence of proteins [57].

3.4.7 Test for terpenoids

A volume of 1 ml sample extract was added to 10 ml of methanol and subjected to shaking. From the mixture 5 ml were taken and mixed with 2 ml of chloroform and then 3 ml of sulphuric acid. A positive result is indicated by the formation of reddish brown colour [57,115].

3.4.8 Test for Quinone

A volume of 1 ml plant extract was treated with concentrated HCl and a yellow precipitate indicates a positive result [114].

3.4.9 Test for flavonoids

A volume of 1 ml plant extract was added to 10 ml of distilled water followed by 5 ml ammonia and then few drops of concentrated H₂SO₄. A positive result is given by a yellow colour [57].

3.4.10 Test for Tannins

By means of a measuring cylinder, 10 ml of distilled water were added to 2 ml of extract while stirring and the mixture was filtered. Exactly 1 ml of ferric chloride was added to the filtrate. Formation of a blue-green precipitate indicates a positive result [113].

3.4.11 Test for alkaloids

Wagner's test was used whereby a volume of 1 ml of the extract was mixed with iodine in potassium iodide. Formation of a cream or reddish precipitate indicates the presence of alkaloids [57].

3.4.12 Test for carbohydrates

A volume of 1 ml of the plant extract was mixed with Benedict's reagent and heated to boil. Brick red precipitate confirms the presence of reducing sugars [116].

3.4.13 Test for Anthraquinones

To a dry test tube, 1 ml of sample extract was placed followed by addition of 10 ml chloroform. The mixture was subjected to shaking for 5 minutes, decanted and the upper part was shaken in ammonia solution. A positive result is indicated by a brick red colour [117].

3.5.0 Nanoparticle Synthesis

3.5.1 Optimization of pH

A volume of 10 ml leaf extract was added to 90 ml of 5 mM aqueous TiCl_4 in a fumehood and pH of the solution was measured. The values of pH were adjusted by adding dilute acid (HCl) or dilute base (NaOH) to the solution. The pH ranges of 5 to 9 were used for the synthesis of TiO_2 NPs over a period of 6 hours at room temperature and their absorbance was measured in wavelength range of 200 – 800 nm.

3.5.2 Optimization of time

Volume of 90 ml (5 mM) aqueous TiCl_4 was mixed with 10 ml leaf extract and the reaction was carried out at pH 7 at room temperature. The absorbance of reactants was measured at 30 minutes interval in a spectral range of 200 – 800 nm over a period of 6 hours.

3.6.0 Experimental Design

Three factors investigated by Central Composite Design (CCD) were aqueous TiCl_4 concentration, X.Caffra volume and Temperature. CCD is an experimental design used to assign the operation factors into a scope of assessment. CCD experimental design lead to a set of 20 experimental runs as shown in table 3.2 below and was used to optimize factors for the synthesis of TiO_2 NPs. The design was constructed using Minitab version 17 and analysis of variance over the quadratic model was conducted with 95 % confidence level.

3.6.1 Response Surface Methodology

The RSM gives the statistical components essential for the assessment of concentration of TiCl_4 , X.Caffra volume and Temperature. The RSM is centred in the development of geometrical models that can predict the response of the factors in the area of assessment. By making use of RSM, independent assessment of each factor and their interaction in this experiment was determined.

Table 3: 1 Experimental Domain values

| Levels | TiCl_4 Concentration (mM) | X.Caffra Volume (ml) | Temperature °C |
|--------|---------------------------------------|-------------------------|-------------------|
| -1 | 3 | 5 | 15 |
| 0 | 6 | 10 | 25 |
| +1 | 9 | 15 | 35 |

Table 3: 2 Experimental Runs

| Run | A:TiCl ₄ <i>Mm</i> | B:X.Caffra <i>Ml</i> | C:Temperature °C | Absorbance <i>a.u</i> |
|-----|----------------------------------|-------------------------|---------------------|--------------------------|
| 1 | 6.00 | 10.00 | 25.00 | |
| 2 | 6.00 | 10.00 | 25.00 | |
| 3 | 9.00 | 15.00 | 35.00 | |
| 4 | 6.00 | 5.00 | 25.00 | |
| 5 | 9.00 | 5.00 | 15.00 | |
| 6 | 6.00 | 10.00 | 15.00 | |
| 7 | 6.00 | 10.00 | 25.00 | |
| 8 | 9.00 | 5.00 | 35.00 | |
| 9 | 9.00 | 15.00 | 15.00 | |
| 10 | 9.00 | 15.00 | 25.00 | |
| 11 | 3.00 | 15.00 | 35.00 | |
| 12 | 6.00 | 10.00 | 25.00 | |
| 13 | 9.00 | 10.00 | 25.00 | |
| 14 | 6.00 | 10.00 | 35.00 | |

Table 3:2 Cont.

| | A: TiCl₄ | B: X. Caffra | C: Temperature | Absorbance |
|----|----------------------------|---------------------|-----------------------|-------------------|
| | <i>mM</i> | <i>ml</i> | °C | <i>a.u</i> |
| 15 | 3.00 | 15.00 | 15.00 | |
| 16 | 6.00 | 10.00 | 25.00 | |
| 17 | 3.00 | 5.00 | 35.00 | |
| 18 | 6.00 | 10.00 | 25.00 | |
| 19 | 3.00 | 10.00 | 25.00 | |
| 20 | 3.00 | 5.00 | 15.00 | |

The experimental methodology was done in accordance with the design where the tests were performed in 250 ml Erlenmeyer flask containing leaf extract and TiCl₄ solution.

3.6.2 Synthesis of TiO₂ NPs

The TiO₂ NPs were synthesised using optimum conditions, filtered from the solution and allowed to dry at 30 °C in an oven. The dried nanoparticles were transferred to a ceramic crucible, placed in a muffle furnace and heated to a temperature of 450 °C for a length of 4 hours. The ceramic crucible was allowed to cool and the obtained particle was taken for characterisation and bioactivity tests.

3.7.0 Characterisation Techniques

3.7.1 Characterising using FTIR

X.Caffra extract was placed on polished KBr plate and allowed to spread over the surface before another plate was mounted on top so that a thin layer of liquid was achieved between the plates. The clamped plates, free from liquid on their edges were analysed in the spectral range of 4000 cm^{-1} - 400 cm^{-1} .

The synthesized TiO_2 NPs were analyzed by FT-IR, 0.0251 g TiO_2 NPs were mixed with dried 2.5003 g KBr and pressed in a sample holder to produce a transparent pellet disk. The disk was analyzed in the spectral range of 4000 cm^{-1} - 400 cm^{-1} .

3.8.0 Bioactivity

Bacteria E.coli was identified and then isolated prior to conducting bioactivity tests by using gram test [118].

3.8.1 Identification tests

Gram staining was done on isolated bacteria in order to differentiate bacteria into two categories, gram positive and gram negative. Gram negative staining was used to identify pathogenic bacteria E.coli [119]

3.8.2 Preparation of culture media

A mass of 55.1002 g powdered nutrient agar was suspended in 1000 ml of distilled water. The solution was heated to boil in order to dissolve the medium completely. The dissolved agar was kept in a tightly closed Pyrex glass bottle and sterilized by autoclaving at $121\text{ }^\circ\text{C}$ for 15 minutes at pressure 15 lbs [120].

3.8.3 Disk Preparation

Whatman filter paper no. 1 was used to prepare disc of 6 mm in diameter and were sterilized in a hot air oven. The prepared discs were then placed in TiO₂ NPs solutions of different concentrations ranging from 10 mg/ml to 80 mg/ml for a period of 18 hours [121].

3.8.4 Culturing of bacteria

The workplace was sterilized by treating it with UV-lamp, methylated spirit and then flamed. A 100 ml of the prepared nutrient agar was poured into petri dishes such that the whole base was totally covered. The media was left to solidify for a period of 15 minutes inside a laminar flow. E.coli was transferred to the prepared petri dishes by means of a loop [122]. Inoculated paper disk in different concentrations of the antibiotics were placed in petri dishes using forceps. The petri dishes were incubated at 37 °C for a period of 24 hours and the zones of inhibitions were observed [60].

3.8.5 Determination of Minimum Inhibitory Concentration (MIC)

Various concentrations of TiO₂ NPs were prepared by serial dilution method ranging from 11 mg/ml to 1 mg/ml. Minimum inhibitory concentration was determined as the lowest concentration of TiO₂ NPs that inhibited the visible growth of E.coli after overnight incubation, by the disk diffusion method [123].

3.8.6 Mean Inhibition Zone

It was determined by the making use of the equation below.

$$\text{mean inhibition diameter} = \frac{\text{sum of all inhibition diameters}}{\text{number of discs used}}$$

3.8.7 Feed Paste Preparation and Bioactivity test

A solution was made by placing 1.0401 g of TiO₂ NPs in 15 ml of distilled water. To the solution, 2.0031 g of broiler starter mesh feed was added and the mixture was subjected to

shaking for 5 minutes, then oven dried at 29 °C for 30 minutes. Feed paste of mass 0.6048 g was placed in 5 ml of distilled water and to the solution, 6 mm disk were inoculated for 18 hours [124]. The disc were transferred to a petri-dish together with the cultured bacteria and a control, using feed without TiO₂ NPs, the prepared petri-dishes were then subjected under U.V light for 30 minutes. After a period of 30 minutes, the petri-dishes were then incubated at 37 °C for 24 hours and the zone of inhibitions were then estimated.

3.8.8 Colony Forming Unity (C.F.U) Bioactivity test

Mass of 0.6052 g of the feed paste was placed in 5 ml of distilled water and the two were sonicated to obtain a homogeneous mixture. From the sonicated mixture, 1 ml was measured and placed in a cuvette, to the cuvette a loop full of bacteria was placed [125]. A control was also prepared were by distilled water without the nanoparticles was mixed with broiler starter mesh feed without antibacterial agent [126]. The cuvettes were then placed in a pyrex glass beak and subjected under UV radiation for 2 hours and the contents were poured in different petri dishes have nutrient agar. Petri dishes were then incubated at 37 °C for 24 hours. The number of viable colony was then calculated, in this case physical counting was done [127].

CHAPTER FOUR

4.0 Introduction

The chapter outlines the results obtained by qualitative analysis of phytochemicals, UV-Vis and FTIR. Results obtained are illustrated in graphs, tables, pictures and are discussed in this chapter.

4.1 Qualitative phytochemical analysis of X.Caffra leaf extract

Table 4.1 gives summary results of the qualitative phytochemicals analysis of the X.Caffra leaf extract which was done.

Table 4: 1 Phytochemical Results of X.Caffra Leaf Extract

| Phytochemical | Observation | Deduction |
|----------------------|---------------------|------------------|
| Terpenoids | Reddish brown | Present |
| Alkaloids | Reddish precipitate | Present |
| Cardiac Glycosides | Reddish brown | Present |
| Phenols | Greenish | Present |
| Saponins | Froth | Present |
| Flavonoids | Yellow precipitate | Present |
| Tannins | Green precipitate | Present |
| Quinones | Yellow color | Present |
| Phlobatannins | Red precipitate | Present |

Table 4: 1 Cont.

| Phytochemicals | Observation | Deduction |
|----------------|-----------------------|-----------|
| Anthraquinones | Deep Red | Present |
| Protein | Deep Purple | Present |
| Carbohydrates | Reddish brown | Present |
| Steroids | Brown color (extract) | Absent |

Qualitative tests done on X.Caffra leaf extract tests indicated the presence of flavonoids, phenols, tannins, aldehydes amides, terpenoids and these phytochemicals are responsible for reduction of titanium ions in solution to form TiO₂NPs. Compared to previously reported work, flavonoids were considered to be absent in X.Caffra leaves while in this research a yellow color was observed when the leaf extract was treated with NH₃ and concentrated H₂SO₄ which indicated the presence of flavonoids [20]. The variation might be due to difference in locations to which the plant leaf samples were collected as plants tend to adapt to the environment by making use of these secondary metabolites [128].

4.2 Optimization of process parameters

4.2.1 Effect of pH

The phytosynthesis reaction was carried out in an initial pH range of 5-9 and pH range was adjusted by adding dilute NaOH or dilute HCl to the solution. After a length of 6 hour the absorbance of the solution were measured at 400 nm and the results are shown in figure 4:1.

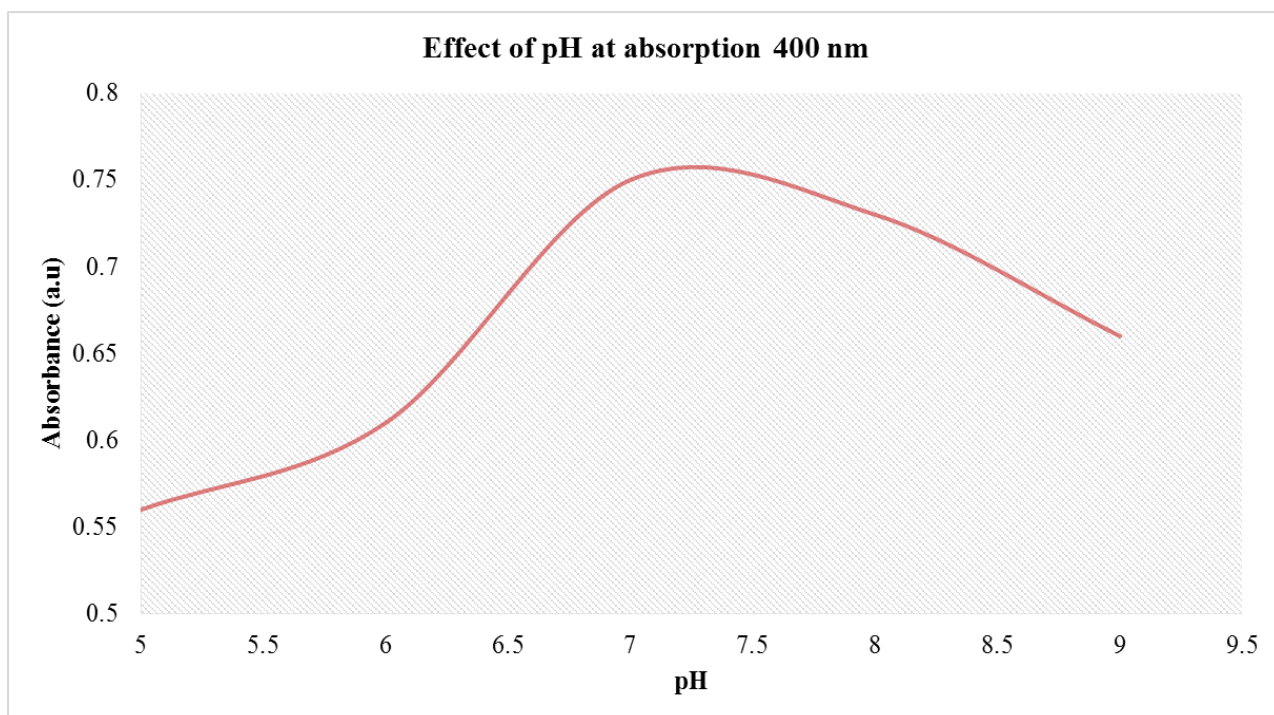


Figure 4: 1 pH Optimization

Optimum initial pH was found to be 7.0. The results suggested that neutral medium is more suitable for the phytosynthesis of TiO_2 NPs than acidic / alkaline pH as rate of hydrolysis of titanium ions were higher at pH 7.0. The results obtained are similar to other works reported before, whereby the neutral pH was found to be the most favorable for the phytosynthesis of TiO_2 NPs [16].

4.2.2 Effect of reaction time

Effect of time was determined by carrying out a reaction at neutral initial pH, temperature was maintained at 25 °C and the absorbance of TiO_2 NPs was measured at 400 nm on 30 minutes intervals.

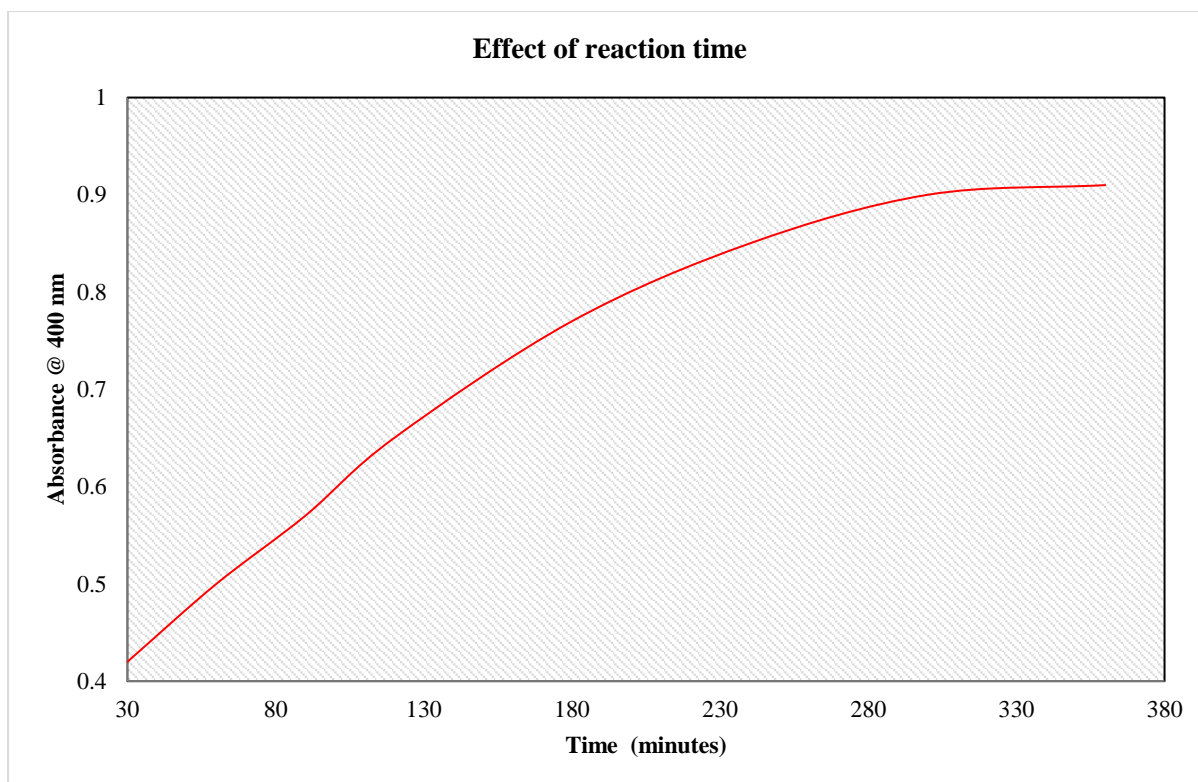


Figure 4: 2 Optimization of Time

After 300 minutes there was no significant increase in absorbance as shown by the graph at 360 minutes which is almost similar to that of 300 minutes. Thus the phytochemical synthesis of TiO₂ NPs reached its maximum at 300 minutes. The maximum amount of time, 300 minutes taken to produce maximum concentration of TiO₂ NPs is more than the previously reported of 240 minutes [129]. The difference in this research might be attributed to the absence of stirring, since stirring increases collision among the reactants hence speeding up the rate of reaction [129].

4.3.0 Characterization

4.3.1 UV-Vis spectra of TiO₂ NPs

The phytosynthesized titanium dioxide nanoparticles were characterized using UV-Vis spectroscopy to determine their structural properties as shown in Figure 4.3. The spectra was plotted as a function of reaction time of TiO₂ NPs. By analyzing the spectra, it was observed

that the maximum absorbance of the phytosynthesized TiO₂ NPs was achieved at close to 400 nm as evident from absorbance spectrum and this peak was attributed to the presence of surface plasmon.

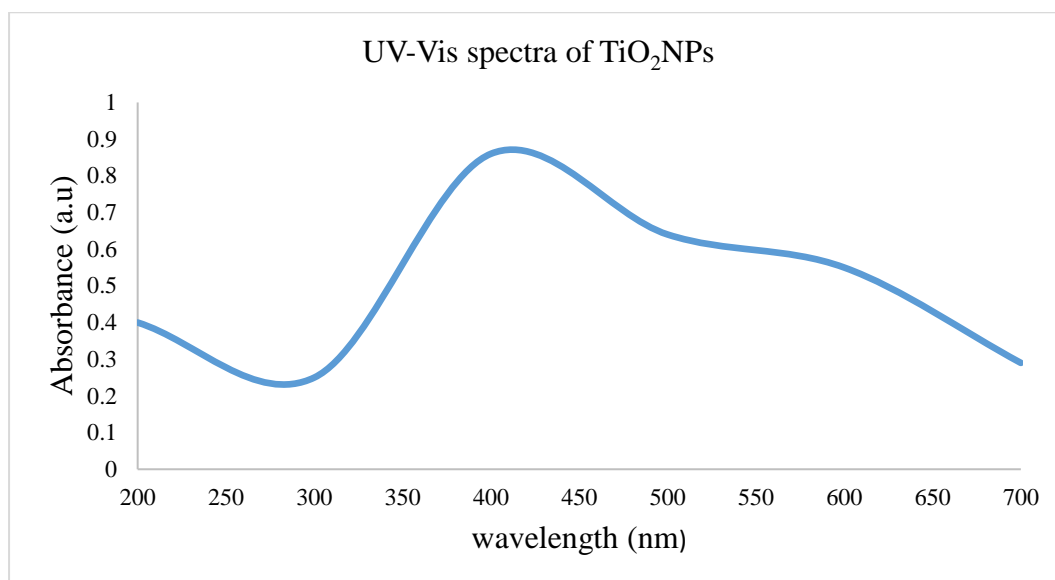


Figure 4: 3 Absorption spectra of TiO₂ NPs in the wavelength range of 300 to 700 nm.

From the graph, the energy responsible for the excitation at maximum peak value can be calculated by making use of equation, $E = hc/\lambda$. Energy value of 3.10 eV is deduced from the calculation and it can be used to substantiate the presence of TiO₂ NPs [18,130]. The spectra peak value obtained is in the range of previously reported wavelength of 387 – 428 nm [18].

4.3.2 FTIR Analysis

FTIR peaks showed two spectrums namely synthesized TiO₂ NPs and X.Caffra leaf aqueous extract. The peaks were given along with the functional groups responsible for the phytosynthesis of the TiO₂ NPs, which could be portrayed to be 3440 cm⁻¹ phenol (O-H stretch), 3109.06 cm⁻¹ carboxylic acids (O-H stretch), 2108.62 cm⁻¹ alkynes and 1075.04 cm⁻¹ (C-O) (stretch alcohols, carboxylic acids, esters). The functional groups depicted acts as capping and stabilizing agents of the phytosynthesized TiO₂ NPs.

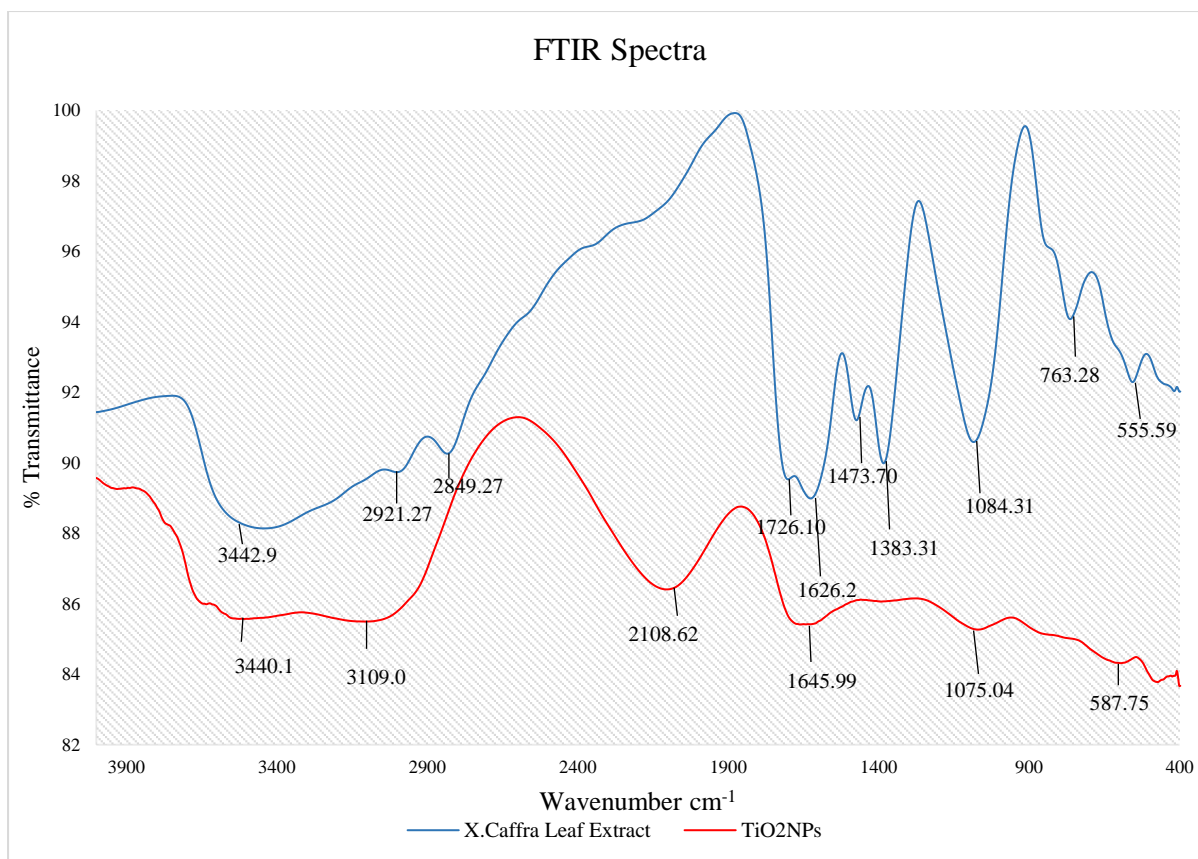


Figure 4: 4 FTIR Spectra of X. Caffra Extract and TiO2 NPS

Aldehyde are reducing agents, their presents in the leaf extract enables the reduction of the titanium ions to produce titanium dioxide nanoparticles. Capping and stabilizing functional groups such as esters, carbohydrates and phenols plays a major role on the effectiveness of TiO₂ NPs as an antibacterial agent. Phenol acts as an antioxidant while the esters and carbohydrates acts as the binding groups [13].

4.4.0 Experimental Design

4.4.1 Experimental analysis

Synthesis and yield of TiO₂ NPs was investigated in the experimental domain which conform to the Central Composite Design in table 3.2. A maximum of 20 experimental runs were conducted in the research in order to optimize the yield of TiO₂ NPs. Six replicates within the design were used to determine the precision of the experimental model. Effects of three

parameters to the yield of TiO₂ NPs produced by green synthetic method were investigated using the design and experimental conditions which were in accordance to the CCD [131].

4.4.2 Method Error

The experimental method was validated by running three replicates within the design and the results obtained were used as a measure to determine consistency of the method.

Table 4: 2 Method Error Results

| Number of runs | <i>mean</i> | <i>standard deviation</i> | $RSD = \frac{100S}{mean}$ |
|-----------------------|--------------------|----------------------------------|---|
| 3 | 0.79 | 0.01 | 1.27 % |

The calculated RSD was 1.27 % which is less than 5 % and this concludes that the method is suitable for the optimization of reaction parameters [131].

4.4.3 CCD (Central Composite Design)

The RSM technique was utilized to fit the experimental results of CCD by using a second order polynomial equation:

$$y = \beta_0 + \beta_1x_1 + \beta_2x_2 + \beta_{12}x_1x_2 + \beta_{11}x_1^2 + \beta_{22}x_2^2 + \varepsilon$$

The model can be used to predict the response at any stated level of the independent variable that is within the experimental domain.

Minitab 17 and Design Expert v. 7.0 tools were used to generate all the experimental conditions based on CCD method, which resulted in 20 experimental conditions. TiO₂ NPs were produced under these conditions and absorbance was measured at 400 nm. The tool was used to perform

all the statistical analysis of the experimental results. A mathematical correlation was derived by applying least squares method to fit a response surface to the measured values of absorbance at specific data of the experimental design matrix.

Table 4: 3 Experimental Matrix with response measured at 400 nm.

| Run | A: TiCl ₄ <i>mM</i> | B: X. Caffra <i>ml</i> | C: Temperature °C | Absorbance <i>a. u</i> |
|-----|-----------------------------------|---------------------------|----------------------|---------------------------|
| 1 | 6.00 | 10.00 | 25.00 | 0.80 |
| 2 | 6.00 | 10.00 | 25.00 | 0.81 |
| 3 | 9.00 | 15.00 | 35.00 | 0.90 |
| 4 | 6.00 | 5.00 | 25.00 | 0.77 |
| 5 | 9.00 | 5.00 | 15.00 | 0.65 |
| 6 | 6.00 | 10.00 | 15.00 | 0.63 |
| 7 | 6.00 | 10.00 | 15.00 | 0.80 |
| 8 | 9.00 | 5.00 | 35.00 | 0.87 |
| 9 | 9.00 | 15.00 | 15.00 | 0.78 |
| 10 | 9.00 | 15.00 | 25.00 | 0.90 |
| 11 | 3.00 | 15.00 | 35.00 | 0.73 |

Table 4.3 Cont.

| Run | A: TiCl ₄ <i>mM</i> | B: X.Caffra <i>ml</i> | C: Temperature °C | Absorbance <i>a.u</i> |
|-----|--|---------------------------------|-----------------------------|--------------------------|
| 12 | 6.00 | 10.00 | 25.00 | 0.80 |
| 13 | 9.00 | 10.00 | 25.00 | 0.90 |
| 14 | 6.00 | 10.00 | 35.00 | 0.82 |
| 15 | 3.00 | 15.00 | 15.00 | 0.58 |
| 16 | 6.00 | 10.00 | 25.00 | 0.80 |
| 17 | 3.00 | 5.00 | 35.00 | 0.75 |
| 18 | 6.00 | 10.00 | 25.00 | 0.80 |
| 19 | 3.00 | 10.00 | 25.00 | 0.73 |
| 20 | 3.00 | 5.00 | 15.00 | 0.50 |

In this research independent variables were coded as **A**, **B** and **C** therefore the second order polynomial equation was given as follows:

$$Y (\text{response}) = \beta_0 + \beta_1 \mathbf{A} + \beta_2 \mathbf{B} + \beta_3 \mathbf{C} + \beta_{12} \mathbf{AB} + \beta_{13} \mathbf{AC} + \beta_{23} \mathbf{BC} + \beta_{11} \mathbf{A}^2 + \beta_{22} \mathbf{B}^2 + \beta_{33} \mathbf{C}^2 \quad [132]$$

Whereby: **Y** is the absorbance, **A** is the concentration of TiCl₄ in mM, **B** is the volume of X.Caffra leaf extract (ml), and **C** Temperature (°C).

The model incorporates linear effects, quadratic effects and two-way interactions between parameters under study. Multiple regression investigation of the experimental results was determined by computation and a second –order polynomial model which defines all the three variables and their association in the phytosynthesis of titanium dioxide nanoparticles was established. The R^2 value is used to express and determine the consistency in the experimental response values which are clarified by the variables and their associations. The model strength is determined by the extent to which a numerical value of R^2 is closer to 1 and in this experiment was 0.9979 [133,134]. A well fitted relationship between the experimental and predicted response values was established on the basis of the R^2 value indicating the suitability of the model for phytosynthesis of TiO_2 NPs. Also the predicted R-Squared value of 0.9881 is in reasonable agreement with the adjusted R-Squared of 0.9950 and this acted as a clear indication that the model is significant for analysis of the response trend.

Table 4: 4 Model fitting test results

| Parameters | Full Quadratic Model | Enhanced Model |
|---------------------------------|-----------------------------|-----------------------|
| R Squared | 0.9989 | 0.9979 |
| Adjusted R Squared | 0.9960 | 0.9950 |
| Predicted R Squared | 0.9740 | 0.9881 |
| <i>p</i> -value for lack-of-fit | 0.0649 | 0.04811 |

By making use of ANOVA results in Table 4.5, the model was bettered with removal of terms having *p*-values greater than 0.05, which are considered as statistically insignificant at a 95 % confidence level. The insignificant term were omitted in the regression analysis.

Table 4: 5 ANOVA table for the full quadratic model.

| Source of Variation | Sum of Squares | Df | Mean Square | F-Value | p-value Prob > F |
|---------------------|------------------------|----|------------------------|---------|------------------|
| Model | 0.220×10^0 | 9 | 0.024×10^0 | 531.62 | < 0.0001 |
| A-TiCl4 | 8.096×10^{-4} | 1 | 8.096×10^{-4} | 18.00 | 0.0017 |
| B-X.Caffra | 2.899×10^{-3} | 1 | 2.899×10^{-3} | 64.45 | < 0.0001 |
| C-Temperature | 0.013×10^0 | 1 | 0.013×10^0 | 286.06 | < 0.0001 |
| AB | 1.050×10^{-3} | 1 | 1.050×10^{-3} | 23.34 | 0.0007 |
| AC | 4.500×10^{-4} | 1 | 4.500×10^{-4} | 10.00 | 0.0101 |
| BC | 5.000×10^{-3} | 1 | 5.000×10^{-3} | 111.15 | < 0.0001 |
| A ² | 1.685×10^{-4} | 1 | 1.685×10^{-4} | 3.75 | 0.0817 |
| B ² | 4.934×10^{-4} | 1 | 4.934×10^{-4} | 10.97 | 0.0079 |
| C ² | 0.017×10^0 | 1 | 0.017×10^0 | 384.88 | < 0.0001 |
| Residual | 4.498×10^{-4} | 10 | 4.498×10^{-5} | | |
| Lack of Fit | 3.665×10^{-4} | 5 | 7.330×10^{-5} | 4.40 | 0.0649 |
| Pure Error | 8.333×10^{-5} | 5 | 1.667×10^{-5} | | |
| Corrected Tot SS | 0.220×10^0 | 19 | | | |

The Model F-value of 531.62 implies that the model is significant and there is only a 0.01 % chance that a Model F-Value this large could occur due to noise. Values of Prob > F less than 0.0500 indicated that the model terms are significant. In this case A, B, C, AB, AC, BC, B², C² are significant model terms making them the limiting factors which, majorly contributes to the appreciation and depreciation of the production rate. The enhanced model is defined by Equation:

$Y_{(TiO_2 NPs\ Synthesis)}$

$$= -0.31 + 0.046A - 0.087B - 1.77C + 0.011AB - 0.023AC - 0.075BC \\ - 0.016B^2 - 0.68C^2$$

This model predicts TiO₂ NPs synthesis using absorbance (a.u) based on three linear effects, three-way interaction and two quadratic effects. Quadratic function of titanium tetrachloride concentration has been found to be negligible in this model. The enhanced model offers a higher prediction capability of 0.9881 for new observations than the full quadratic model of 0.9740.

4.4.4 Effects of measured parameters

Coefficient values for each parameter of the second-order polynomial are expressed in coded units. Coded factors were used in order to eliminate possibilities of pseudo effects which may arise as a result of different in measurement scales [135]. These coefficients are used as a measure of the magnitude of the response resulting from a change in a factor by a unit while other parameters are constant. This explanation is rendered applicable to a range of linear effects over the investigated range of parameters [135]. The model includes an interaction which involves all the three parameters, thus the effect of a change in one parameter associated with the interaction term varies relying on the value chosen for the other parameters

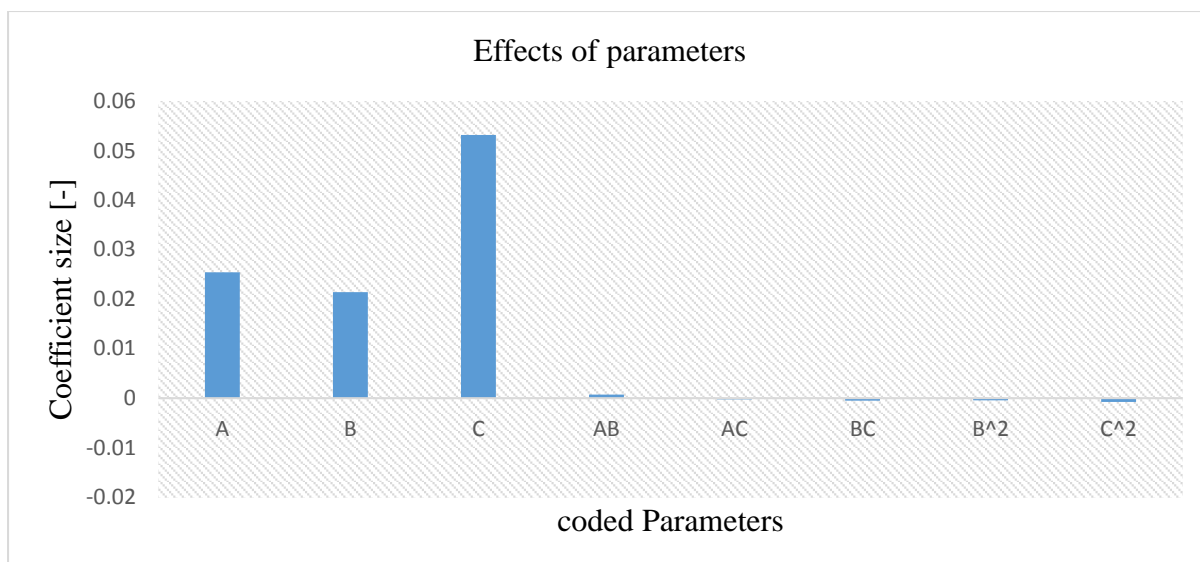


Figure 4: 5 Effects of Coded Parameters

The most significant factor for synthesis of TiO₂ NPs is temperature, this can be explained due to the shift of pH which is dependent on temperature. As the temperature increases, the ionization of hydrogen containing compounds increases and results in the formation of more H⁺ thus the media became acidic. Also at low temperature reacting molecules tend to have less kinetic energy for them to react which result in the low production of TiO₂ NPs. High temperature affects the activity of phytochemicals, bond breaking, function group deactivation and vibrations occurs result in loss of their chemical structure, and thus formation of product is affected.

4.4.5 Method validation

The model appears to fit the data well, it is of great importance to check the model in order to affirm that it offers an estimation with the actual framework [134]. Analyzing and optimizing the fitted model is considered to be erroneous if the model does not show an adequate fit. Normal probability plot is used to ascertain normality of the set of data obtained in the experiment [136].

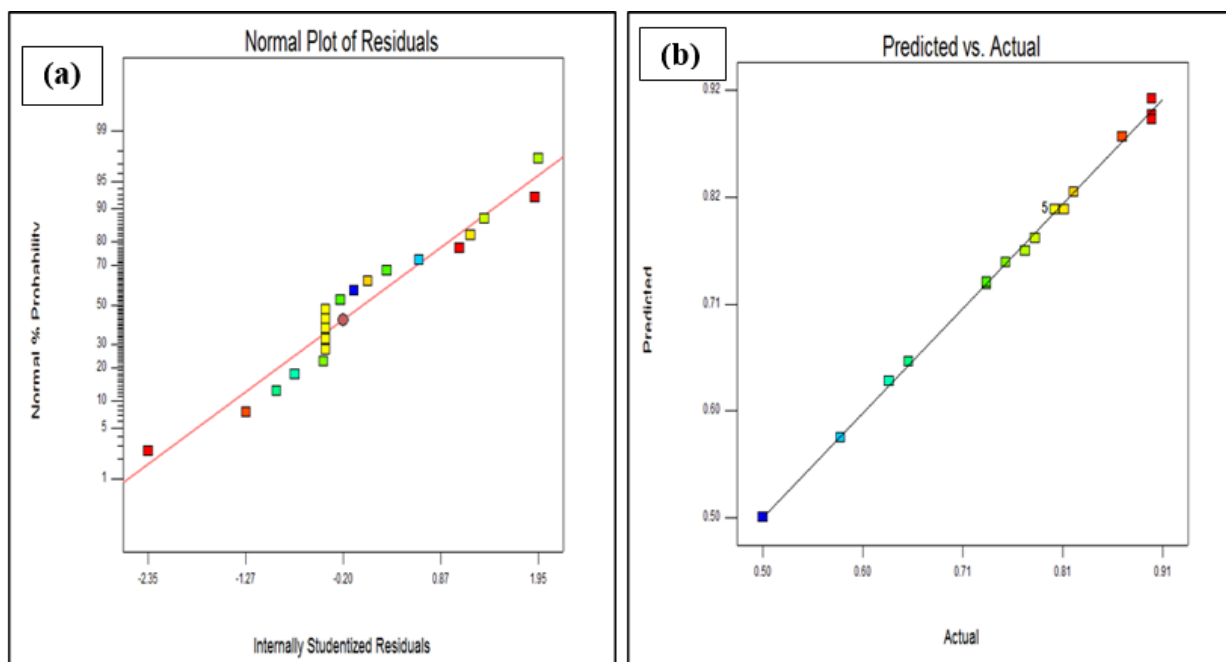


Figure 4: 6 (a) Normal probability plot and (b) predicted vs actual plot

Graphically where residuals are plotted against the normal values of the model shows that all the points are not far away from the diagonal line which entails that the errors are normally dispersed and individual are not externally controlled showing similar deviations indicating a good fitted model. Residuals from the fitted model are normally distributed therefore all the major assumptions of the model have been validated. The plot shown in figure 4: 6 (b) shows a good correlation between the predicted and actual values of responses, thus the model is valid within a given domain for the synthesis of TiO₂ NPs.

4.4.6 Check for outliers

CCD was used to check for outliers on the model and there were no outliers. This depicts the statistical validity of the surface model.

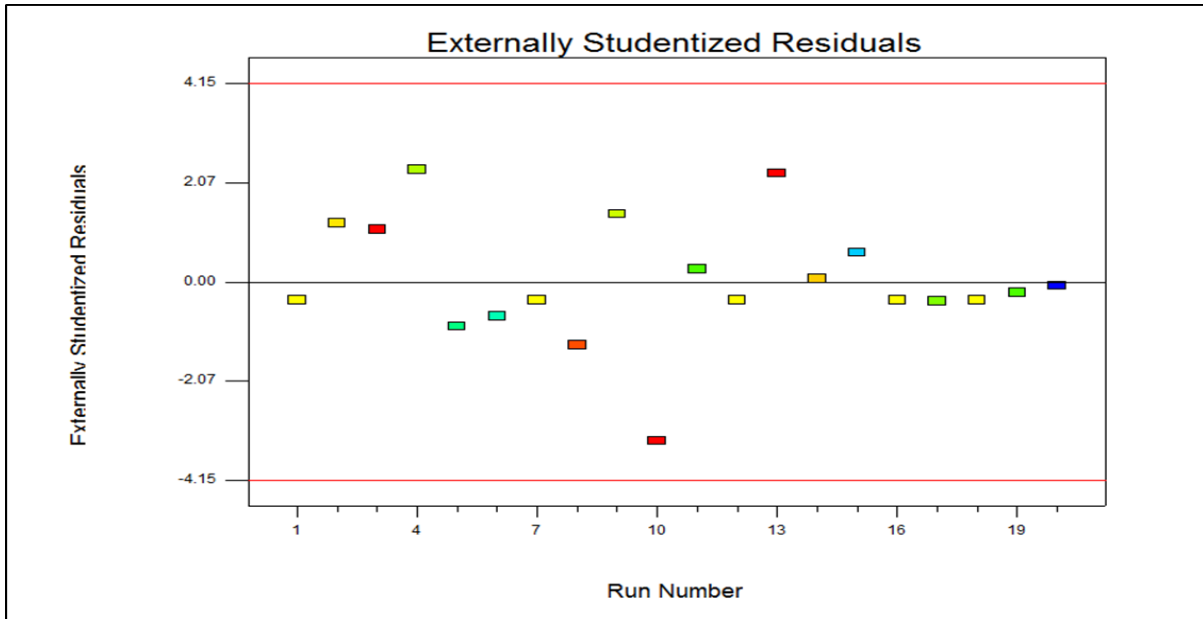


Figure 4: 7 Externally Studentized Residual plot

4.4.7 Surface Response Contour Plots

The interaction effects of the process parameters and their optimal levels are explained using contour plots derived by maintaining one of the variable unchanging at optimum value while the remaining two parameters fluctuates within a defined range.

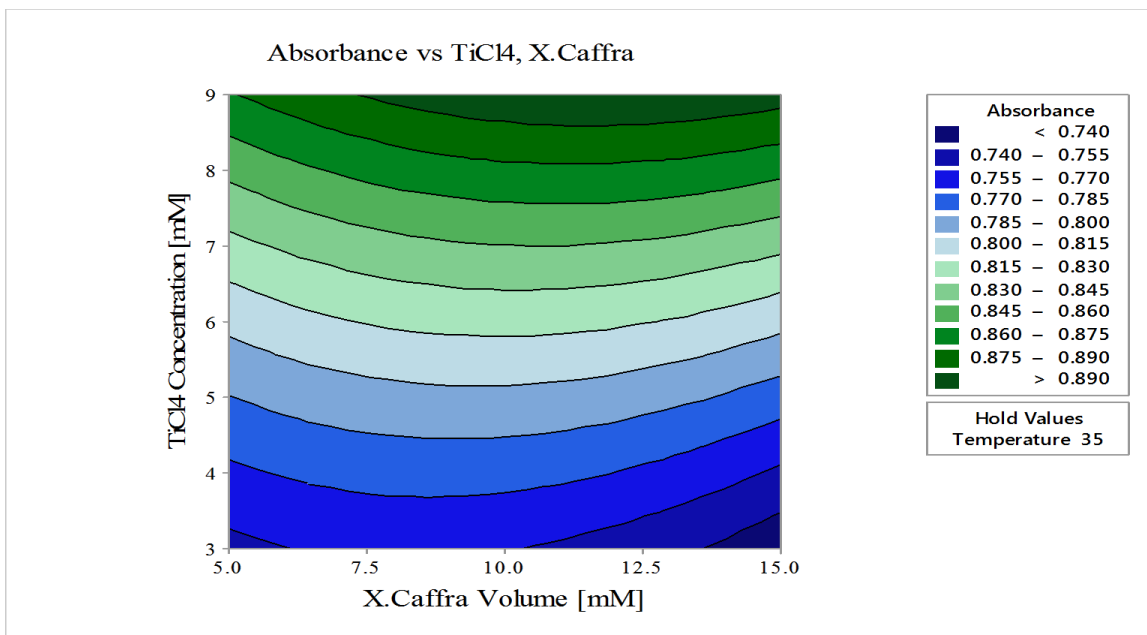


Figure 4: 8 (a) Contour plot of AB (Concentration of TiCl₄ and X.Caffra volume)

Figure 4: 8 shows that at temperature 35 °C, TiCl₄ concentration has more significant effect than X.Caffra volume to the yield of TiO₂ NPs. Initially an increase in X.Caffra volume has a marked increase in the yield of TiO₂ NPs until an optimum volume was attained and the absorbance started to decrease gradually with an increase in leaf extract volume.

The interaction between concentration of titanium chloride and temperature while the volume of extract was held at a constant value of 15 ml is shown in figure 4: 9.

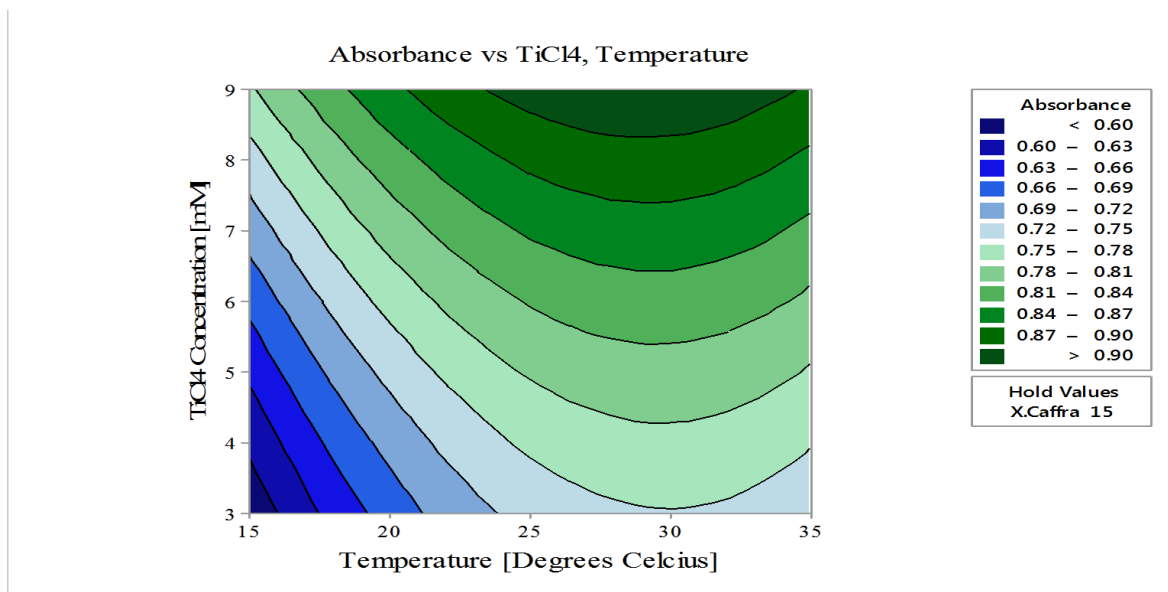


Figure 4: 9 Contour plots of AC (concentration of TiCl₄ and Temperature)

Graphically it is observed that initially as the temperature increases, so does the concentration of TiO₂ NPs. This can be explained by increase in kinetic energy of the molecule as temperature increases making them more reactive as they collide to form TiO₂ NPs. As the temperature increased from approximately 31 °C, the yield of TiO₂ NPs started to decrease and the decrease might be due to reduction in activity of phytochemicals at temperature range outside the norm [137]. As temperature increases, pH values changed to acidic and this can be due to increase in molecular vibration of concentration of hydrogen ion, decreasing its tendency of forming hydrogen bonds, thus leading to low pH value.

Interaction effect of X.Caffra volume and temperature is shown in figure blah. From the contour plot it can be seen that both the parameters were optimized. Optimum volume of X.Caffra was found close to 12 ml and temperature of 33 °C was found to produce optimum concentration of titanium dioxide nanoparticles.

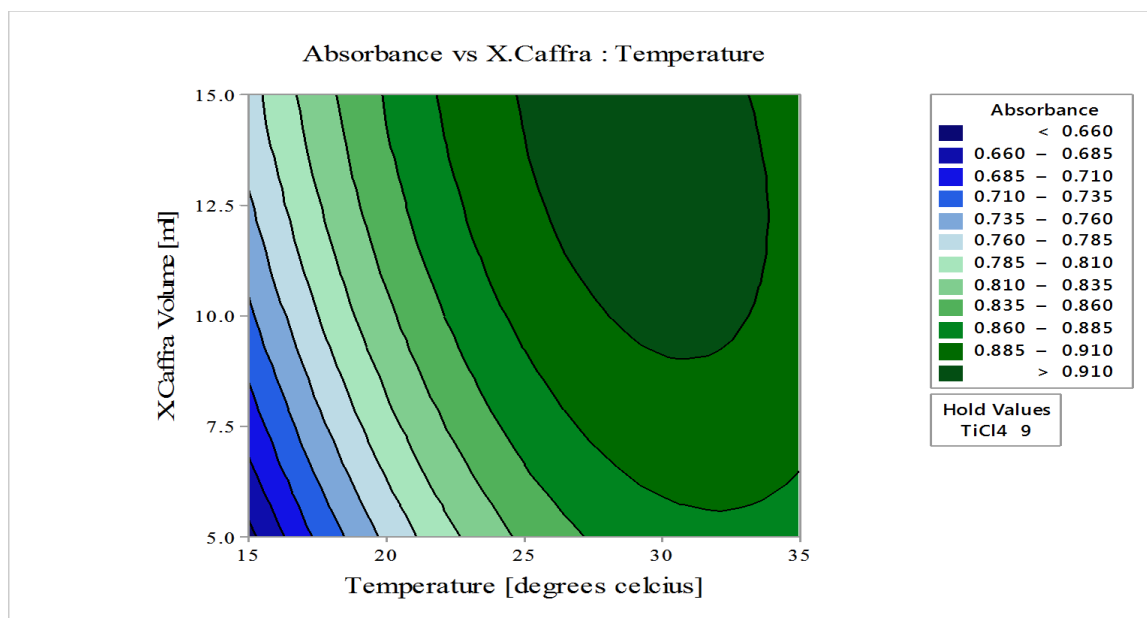


Figure 4: 10 contour plot of BC (X.Caffra and Temperature)

An increase in the leaf extract has a marked increase in the yield of TiO_2 NPs, this is because of increase in the number of molecules that react with titanium ions to form nanoparticles. When approximately 12 ml of leaf extract was added, the production of TiO_2 NPs started to decrease gradually. The decrease is due to the saturation of the solution with the phytochemicals result in decrease in the number of titanium ion thus titanium ions become the limiting factor. Initially, temperature had a strong correlation with the yield of TiO_2 NPs. There was a strong interaction between the volume of X.Caffra and the temperature which is also in sync with F-value of 111.15 obtained. Compared to previously reported work, a room temperature was used for the synthesis of titanium dioxide nanoparticles, though the yield obtained was not considered [129].

4.5.0 Antibacterial Test

4.5.1 Disk Diffusion Method

Bacterial zones of inhibition against pathogenic *E. coli* are indicated by clear zones around paper discs impregnated with antibacterial agents shown in Figure 4.11.

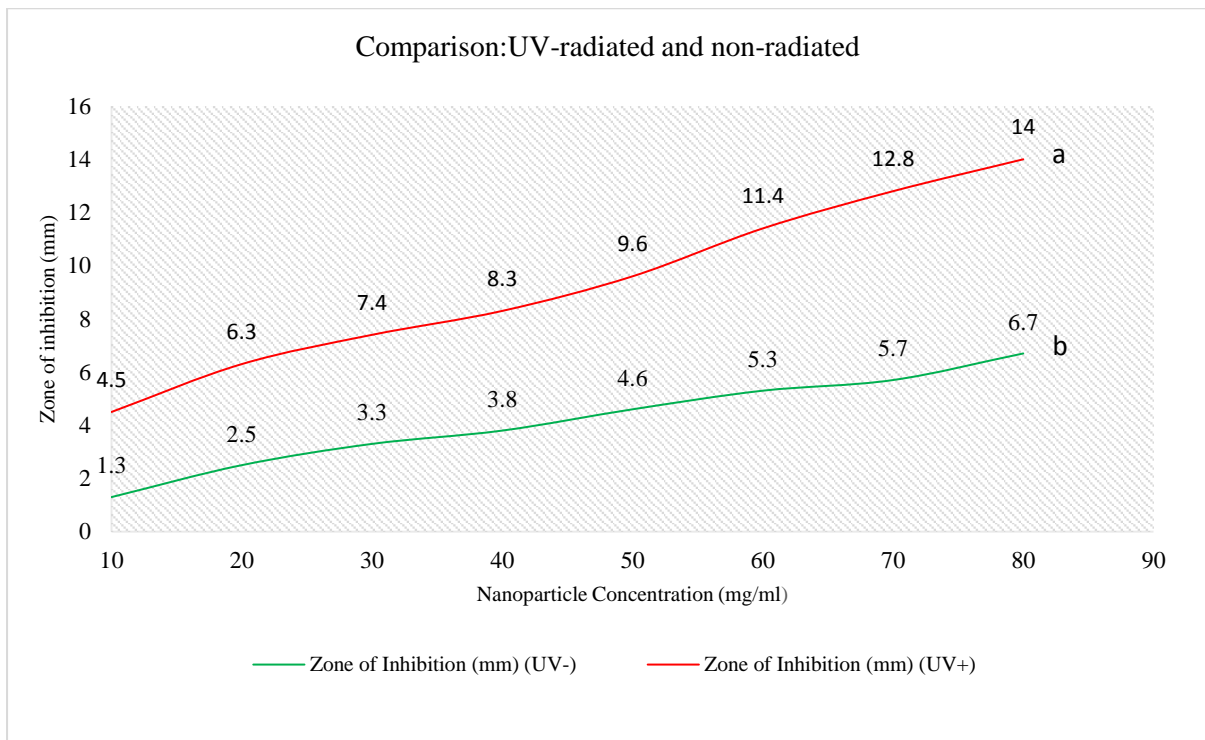
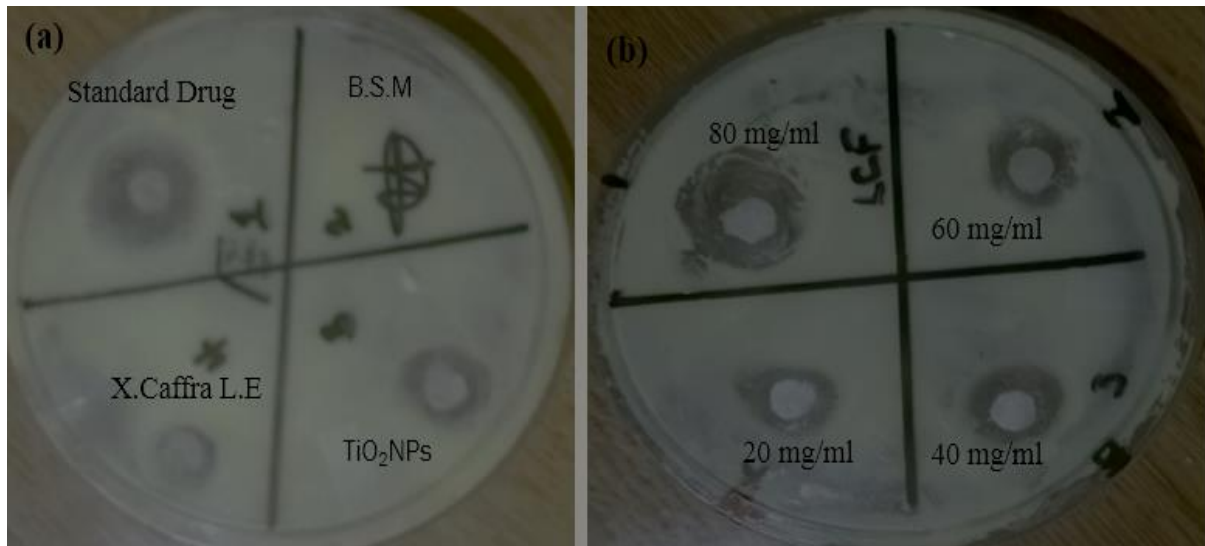


Figure 4: 11 Concentration of Titanium dioxide nanoparticles against zone of inhibition

Effect of different concentrations of TiO₂ NPs on E.coli is given in Figure 4.12 (a) and (b), and it was observed that an increase in concentration of TiO₂ NPs has a marked increase to the zone of E.coli inhibition. This may be explained by increase in contact between pathogenic E.coli and oxidative species generated by TiO₂ NPs [138].

Efficiency of TiO₂ NPs was more pronounced in photocatalytic process as indicated by graph (a) than in non-photocatalytic process, that is, graph (b). The lower activity experienced in the absence of UV radiation is explained to occur as a result of less production of oxidative free radicals which are responsible for the microbial death. The results obtained in figure 4: 11 (a) are in agreement with the previously reported work whereby a linear correlation was reported between concentration of hydroxyl free radicals and inactivation of E. coli in disinfection process using photocatalytic TiO₂ NPs [139].

4.5.2 Colony Forming Unity

Figure 4:12 indicates the number of bacterial E. coli colonies which were able to grow after subjected under UV radiation.

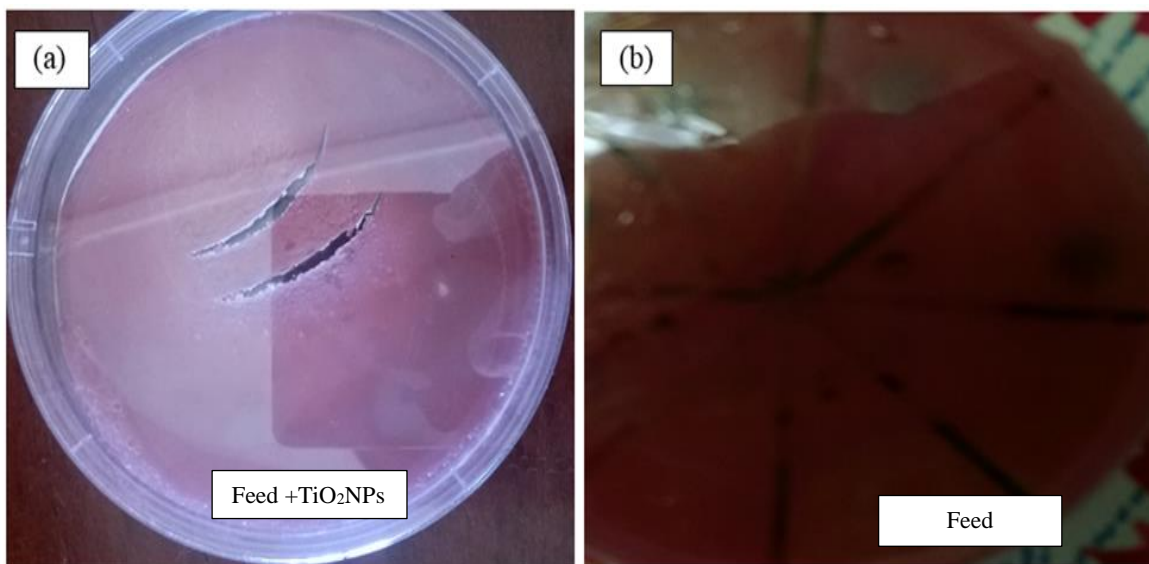


Figure 4: 12 Colony Forming Unit

A pronounced decrease in the number of viable bacteria was observed on the UV-radiated TiO₂ NPs-feed, demonstrating photo-killing activity. The percentage reduction of pathogenic E.coli may be described by considering the charge on bacterial cell wall. The bacterial cell walls are reported to be negatively charged and causes lipids to react with free metal ions in solution. The existence of charge difference between bacteria and the titanium metal ion creates an electromagnetic attraction between the bacteria and treated feed. TiO₂ NPs are proposed to release ions, which react with electron donating groups such as thiols (-SH) of the protein present on pathogenic E.coli cell wall [139]. Protein projectiles on the cell membrane of bacteria facilitates the uptake of nutrients via cell wall, so by deactivating them, results in a decrease to the membrane permeability to nutrients and eventually cellular death occurs. Once enough amounts of nanoparticles bind to the bacterium cell wall, membrane fluidity would be affected and that leads to decomposition of membrane phospholipid structure, decrease in its hydrophobic properties followed by bacterial death. It is also proposed that, TiO₂ NPs causes peroxidation of polycyclic phospholipid compounds of bacterial membrane and reduce the membrane properties, membrane dependent respiratory function and lastly cell death occurs [140].

4.5.3 Minimum Inhibitory Concentration

Concentration ranging from 1-11 mg/ml of TiO₂ NPs and the paper disk were inoculated for 18 hours in the solution. The bacteria was spread on an Ager and inoculated disk in different concentrations were transferred and placed on cultured bacteria. The MIC was determined as the least concentration where there was an observable zone of inhibition and results are shown in figure 4.13.

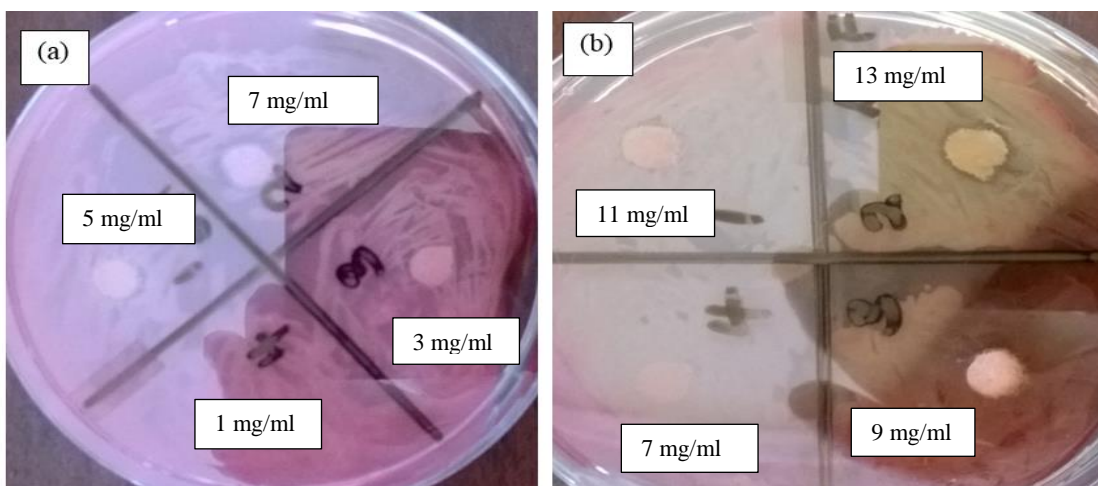


Figure 4: 13 Minimum Inhibitory Concentration

The MIC obtained for both TiO₂ NPs and feed containing TiO₂ NPs were found to be 5 mg/ml and 11 mg/ml respectively. The MIC obtained for TiO₂ NPs compared to other previously reported work, is of average magnitude. The small differences might be due to the effect of particle size and shape, as smaller particles ranging from 2-10 nm are said to be more effective than large particles [141]. The nanoparticles incorporated in feed has a lower MIC value which indicates that less prepared feed is required for inhibiting growth of the organism [142]. The calculated t-test value in Appendix C indicated that there is a significant difference between TiO₂NPs in the absence of UV and standard drug, while there is no significant difference in the presence of UV.

CHAPTER FIVE

CONCLUSION AND RECOMMENDATIONS

5.1 Conclusion

- ❖ TiO₂NPs were successfully synthesized with optimum conditions being initial pH of 7, reaction time 300 minutes, extract volume 11 ml, 9 mM of TiCl₄ and temperature of 33 °C.
- ❖ The investigated parameters indicated that temperature has greatest effect on the synthesis of TiO₂ NPs.
- ❖ Maximum absorption peak under UV-Vis of the synthesized TiO₂ NPs is centered at 400 nm.
- ❖ Phenols (O-H stretch) 3440.13 cm⁻¹, carboxylic acid (O-H) 3109.06 cm⁻¹, alkynes 2108.62 cm⁻¹ and C-O (stretch alcohols, carboxylic acids, esters) 1075.04 cm⁻¹.
- ❖ The synthesised TiO₂ NPs exhibits maximum antibacterial activity under UV-radiation
- ❖ Green synthesized TiO₂ NPs provides a promising approach that satisfies photocatalytic killing of pathogenic E.coli.

5.2 Recommendations

- ❖ Pharmacokinetic and pharmacodynamics studies to be conducted on the synthesized nanoparticles to establish the baseline toxicity level.
- ❖ Other experimental designs and different statistical tools must be used to investigate the interaction of the above parameters
- ❖ Antioxidant activity, total phenolic content and DPPH radical scavenging assay to be investigated on the synthesized TiO₂ NPs.

REFERENCE

- [1] Muchadeyi FC, Wollny CBA, Eding H, Weigend S, Makuza SM, Simianer H. Variation in village chicken production systems among agro-ecological zones of Zimbabwe. *Trop Anim Health Prod* 2007;39:453–61. doi:10.1007/s11250-007-9050-0.
- [2] Ellen, Tze E. Characterisation of *Escherichia coli* Isolated From Village Chicken and Soil Samples. University of Malaysia Sara Waka, 2011.
- [3] Nandi S, Maurer JJ, Hofacre C, Summers AO. Gram-positive bacteria are a major reservoir of Class 1 antibiotic resistance integrons in poultry litter. *Natl Acad Sci* 2004;101:1–5.
- [4] Msotte PL, Cardona CJ. *Poultry Disease Handbook for Africa*. first. California: The Global Livestock Collaborative Research Support Program; 2009.
- [5] Chinyemba F. Agricultural information, urban farmers, poultry farming, libraries, animal agricultural information systems; open access 1. *Columbus IFLA* 2016:1–11.
- [6] Gueye F. Ethnoveterinary medicine against poultry diseases in African villages. *Worlds Poult Sci J* 1999;55:187–98. doi:10.1079/WPS19990013.
- [7] Tablante, Nathaniel L RMTSLTDABKP. Descriptive study of the microbial profile of poultry litter from broiler farms with and without a history of gangrenous dermatitis and litter from an experimental poultry house. *Poult Sci Assoc* 2013;22:344.350. doi:<https://doi.org/10.3382/japr.2012-00593>.
- [8] Elumalai K, Velmurugan S, Ravi S, Kathiravan V, Ashokkumar S. Green synthesis of zinc oxide nanoparticles using *Moringa oleifera* leaf extract and evaluation of its antimicrobial activity. *Spectrochim Acta - Part A Mol Biomol Spectrosc* 2015;143:158–64. doi:10.1016/j.saa.2015.02.011.

- [9] Sundrarajan M, Gowri S. Green synthesis of titanium dioxide nanoparticles by *nyctanthes arbor-tristis* leaves extract. *Chalcogenide Lett* 2011;8:447–51.
- [10] Salam HA, Sivaraj R. *Ocimum basilicum* L. var. *purpurascens* Benth Lamiaceae Mediated Green Synthesis and Characterization of Titanium Dioxide Nanoparticles. *Adv Biores* 2014;5:10–6. doi:10.15515/abr.0976-4585.5.3.1016.
- [11] Abdul J., Nuaman R. and, Aham A. Biological synthesis of Titanium Dioxide nanoparticles by *Curcuma longa* plant extract and study its biological properties. *World Scie* 2016;49:204–22.
- [12] Ismagilov Z., Tsykoza L., Shikina N., Zarytova V., Zinoviev V. and, Zagrebelnyi S. Synthesis and stabilization of nano-sized titanium dioxide 2009;78. doi:10.1070/RC2009v078n09abeh004082.
- [13] Santhoshkumar T, Rahuman A, Jayaseelan C, Rajakumar G, Marimuthu S, Kirthi A, et al. Green synthesis of titanium dioxide nanoparticles using *Psidium guajava* extract and its antibacterial and antioxidant properties. *Asian Pac J Trop Med* 2014;7:968–76. doi:10.1016/S1995-7645(14)60171-1.
- [14] Sharma A, Karn R. and, Pandiyan S. Synthesis of TiO₂ Nanoparticles by Ultrasonic Assisted Sol-Gel Method. *J Basic Appl Eng Res* 2013;5:2970–4.
- [15] Sinica D. and, Annadurai G. Pelagia Research Library Novel eco-friendly synthesis of titanium oxide nanoparticles by using *Planomicrobium* sp . and its antimicrobial evaluation. *Der Pharm* 2013;4:59–66.
- [16] Khadar A, Behara D and, Kumar M. Synthesis and Characterization of Controlled Size TiO₂ Nanoparticles via Green Route using *Aloe vera* Extract. *Int J Sci Res* 2016;5:1913–6.

- [17] Kharissova O, Dias H, Kharisov B, Prez B and, Victor M. The greener synthesis of nanoparticles. *Trends Biotechnol* 2013;31:240–8. doi:10.1016/j.tibtech.2013.01.003.
- [18] Sivaranjani V and, Philominathan P. Synthesize of Titanium dioxide nanoparticles using *Moringa oleifera* leaves and evaluation of wound healing activity. *Wound Med* 2016;12:1–5. doi:10.1016/j.wndm.2015.11.002.
- [19] Parra R, Góes M, Castro M, Longos E, Bueno P and, Varela J. Reaction pathway to the synthesis of anatase via the chemical modification of titanium isopropoxide with acetic acid. *Chem Mater* 2008;20:143–50. doi:10.1021/cm702286.
- [20] Munodawafa T. Screening of some traditional medicinal plants from Zimbabwe for biological and anti-microbial activity. University of Zimbabwe, 2012. doi:10.1.1.1026.2276.
- [21] Zengeni T. The competitiveness and performance of the Zimbabwe poultry industry. *Jr Reseach Ccred* 2015:1–28.
- [22] Deliwe T, Chisango F and, Kwesu I. Assessment of Entrepreneurial Skills for Smallholder Broiler Producers in Zimbabwe: A Case of Mazowe District in Mashonaland Central Province. *Int J Sci Technol* 2015;3:235–40.
- [23] Bukenya-Ziraba R and, Kamoga D. An inventory of medicinal plants used in treating poultry diseases in Jinja district, eastern Uganda. *Afr J Ecol* 2007;45:31–8. doi:10.1111/j.1365-2028.2007.00854.x.
- [24] Chikangaidze S. Analysis of the Regional Competitiveness of Zimbabwe’s Broiler Enterprises. University of Zimbabwe, 2011.
- [25] Ram P, Vivek K and, Kumar S. Nanotechnology in sustainable agriculture: Present concerns and future aspects. *African J Biotechnol* 2014;13:705–13.

doi:10.5897/AJBX2013.13554.

- [26] Huang A, Lin T and, Wu C. Antimicrobial Susceptibility and Resistance of Chicken *Escherichia coli* , *Salmonella* spp ., and *Pasteurella multocida* Isolates Published by : American Association of Avian Pathologists content in a trusted digital archive . *Indian J Med Microbiol* 2014;53:100–13.
- [27] Huang T, Lin T and, Wu C. Antimicrobial susceptibility and resistance of chicken *Escherichia coli*, *Salmonella* spp., and *Pasteurella multocida* isolates. *Indian J Med Microbiol* 2009;53:89–93. doi:10.1637/8268-021608.
- [28] Orwa C, Mutua A, Kindt R and, Simons A. Agroforestry Database:a tree reference and selection guide version 4.0. *Agroforestry Database* 2009;0:1–5.
<http://www.worldagroforestry.org/af/treedb/> (accessed October 20, 2016).
- [29] Taylor P, Chibememe G, Muboko N, Gandiwa E, Kupika OL, Victor K and, et al. Embracing indigenous knowledge systems in the management of dryland ecosystems in the Great Limpopo Transfrontier Conservation Area : the case of Chibememe and Tshovani communities , Chiredzi , Zimbabwe. *Int J Environ Res Public Health* 2014;37–41. doi:10.1080/14888386.2014.934715.
- [30] Tsuang Y, Sun J, Huang Y, Lu C, Chang W, Wang C. Studies of photokilling of bacteria using titanium dioxide nanoparticles. *Adv Nat Sci Nanosci Nanotechnol* 2008;32:167–74. doi:10.1111/j.1525-1594.2007.00530.
- [31] Syed N, Zahir S, Khan M and, Muzaffar A. Hazardous Effects of Titanium Dioxide Nanoparticles in Ecosystem. *Bioinorg Chem Appl* 2017;2017:12.
doi:org/10.1155/2017/4101735.
- [32] Mahmood A. *Handbook of Nanoparticles*. Tehran, Iran: Springer International

- Publishing; 2015. doi:10.1007/978-3-319-13188-7.
- [33] Sanchez-Botero L, Herrera AP and, Hinestroza JP. Oriented Growth of α -MnO₂ Nanorods Using Natural Extracts from Grape Stems and Apple Peels. *J Nanomater* 2017;117:2–15. doi:doi:10.3390/nano7050117.
- [34] Wilson D. Surface Coatings. In: Harvard J, editor. *Surf. Coatings*. Second Edi, New York, USA: Elsevier Science Publishing Co. Inc.; 1988, p. 15–27.
- [35] Heaney P, Banfield J. Structure and chemistry of silica, metal oxides, and phosphates. *Mineral Soc Am* 1993;28:185–233.
- [36] Koparde N. Study of Titanium Dioxide Nanoparticles. *J Mater Chem* 2006;1:1–45. doi:hj256-456-45656.
- [37] West R and, Henry C. Modelling the Chloride Process for Titanium Dioxide Synthesis. *Int J Mod Chem Appl Sci* 2008. doi:10.1021/jp0661950.
- [38] Rogers B, Jesse A and, Pennathur S. *Nanotechnology Understanding Small System*. Third. New York: Taylor and Francis; 2014.
- [39] Poinern G. *A Laboratory Course in Nanoscience and Nanotechnology*. Second. New York: Taylor and Francis; 2014.
- [40] Cláudia GC. *Synthesis , Spectroscopy and Characterization of Titanium Dioxide Based Photocatalysts for the Degradative Oxidation of Organic Pollutants*. University of Porto, 2008.
- [41] Weigend S. *Titanium Dioxide Nanomaterials*. vol. 26. second. New York: Taylor and Francis; 2011. doi:12.141.142.36.
- [42] Mahmood A. *Handbook of Nanoparticles*. Tehran, Iran: Springer International

- Publishing; 2015. doi:10.1007/978-3-319-13188-7.
- [43] Namita R. Methods of preparation of Nanoparticles. *Int J Adv Eng Technol* 2015;7:1806–11. doi:22311963.
- [44] Stride JA, Tuong NT. Controlled Synthesis of Titanium dioxide nanostructures 2 . *Properties of Titanium Dioxide* 2010;162:261–94.
doi:10.4028/www.scientific.net/SSP.162.261.
- [45] Theivasanthi T and, Alagar M. Titanium dioxide (TiO₂) Nanoparticles XRD Analyses: An Insight. *J Chem Technol Biotechnol* 2013;12:100–210.
- [46] Shah M, Fawcett D, Sharma S, Tripathy S and, Poinern G. Green synthesis of metallic nanoparticles via biological entities. *Int J Mater* 2015;8:7278–308.
doi:10.3390/ma8115377.
- [47] Ganapathy S and, Siva K. Bio-synthesis, Characterisation and Application of Titanium Oxide Nanoparticles by *Fusarium oxysporum*. *Int J Life Sci Res* 2016;4:69–75.
- [48] Khan N, Jameel N and, Rehman S. Optimizing Physioculture Conditions for the Synthesis of Silver Nanoparticles from *Asperillus niger*. *J Nanomedicine Nanotechnol* 2016;7:7–10. doi:10.4172/2157-7439.1000402.
- [49] Mboniyirivuze A, Zongo S, Diallo A, Bertrand S, Minani E. Titanium Dioxide Nanoparticles Biosynthesis for Dye Sensitized Solar Cells application : Review. *Phys Mater Chem* 2015;3:12–7. doi:10.12691/pmc-3-1-3.
- [50] Vadakkan K, Kannan VR. *International Journal of Current Research and Academic Review* 2015;3:334–42.
- [51] Mendelson M. *Learning Bio-Micro-Nanotechnology*. First Edit. New York: Taylor and Francis; 2013.

- [52] Rajakumar G, Rahuman A and, Jayaseelan C. Solanum trilobatum extract-mediated synthesis of titanium dioxide nanoparticles to control *Pediculus humanus capitis*, *Hyalomma anatolicum anatolicum* and *Anopheles subpictus*. *Indian J Med Microbiol* 2013;12:188–200. doi:10.1007/s00436-013-3676-9.
- [53] Zhao L, Liu D and, Wang X. Effect of several factors on peracetic acid pretreatment of sugarcane bagasse for enzymatic hydrolysis. *J Chem Technol Biotechnol* 2007;82:1115–21. doi:10.1002/jctb.
- [54] Vardhini B, Naseem J and, Haleemkhan A. Synthesis of Nanoparticles from Plant Extracts. *Int J Mod Chem Appl Sci* 2015;2:195–203. doi:2349-0594.
- [55] Narayanan K and, Sakthivel N. Green synthesis of biogenic metal nanoparticles by terrestrial and aquatic phototrophic and heterotrophic eukaryotes and biocompatible agents. *Adv Colloid Interface Sci* 2011;169:59–79. doi:10.1016/j.cis.2011.08.004.
- [56] Singh R, Nawale LU, Arkile M, Shedbalkar UU, Wadhvani SA, Sarkar D, et al. Chemical and biological metal nanoparticles as antimycobacterial agents: A comparative study. *Int J Antimicrob Agents* 2015;46:183–8. doi:10.1016/j.ijantimicag.2015.03.014.
- [57] Saxena M, Saxena J, Nema R, Singh D and, Gupta A. Phytochemistry of Medicinal Plants. *J Pharmacogn Phytochem Phytochem* 2013;1:168–82. doi:2668735-5.
- [58] Pandey S and, Abhay K. Chemistry and Biological Activities of Flavonoids: An Overview. *Sci World J* 2013;2013:16. doi:10.1155.
- [59] Robbins RJ. Phenolic Acids in Foods : An Overview of Analytical Methodology *Phenolic Acids in Foods : An Overview of Analytical* 2003;51:2866–87. doi:10.1021/jf026182t.

- [60] Marles J. and, Shahriar K. Monocyclic Phenolic Acids; Hydroxy- and Polyhydroxybenzoic Acids: Occurrence and Recent Bioactivity Studies. *Molecules* 2010;15:7985–8005. doi:doi:10.3390.
- [61] Silva E, Souza J, Rogez H, Rees J. and, Larondelle Y. Antioxidant activities and polyphenolic contents of fifteen selected plant species from the Amazonian region. *Food Chem* 2007;101:1012–8.
- [62] Venket RA and, Leticia R. *Phytochemicals Isolation , Characterisation and Role in Human Health*. New York: AvE4EvA MuViMix Records; 2015.
- [63] Saxena M, Saxena J, Pradhan A. Review Article 2012;16:130–4.
- [64] Song CE. An Overview of Cinchona Alkaloids in Chemistry. *Int Food Res J* 2009;11:1–10.
- [65] Roopan S, Bharathi A, Prabhakarn A, Abdul A, Velayutham K, Rajakumar G, et al. Efficient phyto-synthesis and structural characterization of rutile TiO₂ nanoparticles using *Annona squamosa* peel extract. *Spectrochim Acta - Part A Mol Biomol Spectrosc* 2012;98:86–90. doi:10.1016/j.saa.2012.08.055.
- [66] Velayutham K, Rahuman A, Rajakumar G, Santhoshkumar T, Marimuthu S, Jayaseelan C, et al. Evaluation of *Catharanthus roseus* leaf extract-mediated biosynthesis of titanium dioxide nanoparticles against *Hippobosca maculata* and *Bovicola ovis*. *Parasitol Res* 2012;111:2329–37. doi:10.1007/s00436-011-2676-x.
- [67] Surendiran A, Sandhiya S, Pradhan SC, Adithan C. Novel applications of nanotechnology in medicine 2009:689–701.
- [68] Karunaratne N. Nanotechnology in Medicine. *J Natl Sci Found* 2007;3:149–52.
- [69] Cavalcanti A, Shirinzadeh B and, Kretly L. Medical nanorobotics for diabetes control.

- J Exp Nanosci 2008;4:127–38. doi:10.1016/j.nano.2008.03.001.
- [70] Wilczewska A, Niemirowicz K, Markiewicz K, Halina C. Nanoparticles as drug delivery systems. Eur J Pharmacol 2012;64:1864–1882. doi:10.1016/S1734-1140(12)70901-5.
- [71] Pandey R, Ahmad Z, Sharma S, Khuller GK. Nano-encapsulation of azole antifungals: Potential applications to improve oral drug delivery. Int J Pharm 2005;301:268–76. doi:10.1016/j.ijpharm.2005.05.027.
- [72] Beg S, Rizwan M, Sheikh AM, Hasnain MS, Anwer K, Kohli K. Advancement in carbon nanotubes: Basics, biomedical applications and toxicity. J Pharm Pharmacol 2011;63:141–63. doi:10.1111/j.2042-7158.2010.01167.x.
- [73] Moon E, Yi G, Kang J, Lim J, Kim H and, Pyo S. An increase in mouse tumor growth by an in vivo immunomodulating effect of titanium dioxide nanoparticles. J Immunotoxicol 2011;8:56–67. doi:10.3109/1547691X.2010.543995.
- [74] Chen E, Ruvalcaba M, Araujo L, Chapman R, Chin W-C. Ultrafine titanium dioxide nanoparticles induce cell death in human bronchial epithelial cells. J Exp Nanosci 2008;3:171–83. doi:10.1080/17458080802412430.
- [75] Sha B, Gao W, Han Y, Wang S, Wu J, Xu F, et al. Potential Application of Titanium Dioxide Nanoparticles in the Prevention of Osteosarcoma and Chondrosarcoma Recurrence. J Nanosci Nanotechnol 2013;13:1208–11. doi:10.1166/jnn.2013.6081.
- [76] Ahmad R and, Meryam S. Titanium Dioxide nanoparticles as an antibacterial agent against E. coli. Int J Innov Res Sci Eng Technol 2013;2:3569–74.
- [77] Hirakawa K. Fundamentals of Medicinal Application of Titanium Dioxide Nanoparticles. Nanoparticles Technol., Shizuoka, Japan: InTech; 2016, p. 2–21.

doi:<http://dx.doi.org/10.5772/61302>.

- [78] Schleh C, Muehlfeld C, Pulskamp K, Schmiedl A, Nassimi M, Lauenstein HD, et al. The effect of titanium dioxide nanoparticles on pulmonary surfactant function and ultrastructure. *Respir Res* 2009;10:90. doi:10.1186/1465-9921-10-90.
- [79] Mosaddeghi H, Rezaei B, Mosaddeghi H. Applications of Titanium Dioxide Nanoparticles. In: Behzad R, editor. *Appl. Titan. Dioxide Nanocoatings*, Isfahan: ResearchGate; 2009, p. 1–4. doi:10.13140/RG.2.1.2184.6006.
- [80] Gong P, Li J, Chi W, Wang J, Yao T, Zhang K, et al. Variants in COMT and DBH influence on response inhibition ability in Chinese Han females. *Cell Mol Neurobiol* 2011;31:1163–9. doi:10.1007/s10571-011-9717-y.
- [81] Babaei E, Dehnad A, Hajizadeh N, Valizadeh H and, Reihani S. A study on Inhibitory Effects of Titanium Dioxide Nanoparticles and its Photocatalytic Type on *Staphylococcus aureus*, *Escherichia coli* and *Aspergillus flavus*. *Appl Food Biotechnol* 2016;3:115–23.
- [82] Hassan M, Amna T, Al-Deyab S, Kim H, Oh T and, Khil M. Toxicity of Ce₂O₃/TiO₂ composite nanofibers against *S. aureus* and *S. typhimurium*: A novel electrospun material for disinfection of food pathogens. *Colloids Surfaces A Physicochem Eng Asp* 2012;415:268–73. doi:10.1016/j.colsurfa.2012.08.058.
- [83] Srikanth K, Pereira E, Duarte AC, Ahmad I, Rao JV. Assessment of cytotoxicity and oxidative stress induced by titanium oxide nanoparticles on Chinook salmon cells. *Environ Sci Pollut Res* 2015;22:15571–8. doi:10.1007/s11356-015-4740-z.
- [84] Mahmood M, Casciano DA, Mocan T, Iancu C, Xu Y, Mocan L, et al. Cytotoxicity and biological effects of functional nanomaterials delivered to various cell lines. *J*

- Appl Toxicol 2010;30:74–83. doi:10.1002/jat.1475.
- [85] Marciano FR, Lima-Oliveira DA, Da-Silva NS, Diniz A V., Corat EJ, Trava-Airoldi VJ. Antibacterial activity of DLC films containing TiO₂ nanoparticles. J Colloid Interface Sci 2009;340:87–92. doi:10.1016/j.jcis.2009.08.024.
- [86] Othman S, Raudhah N, Salam A, Zainal N, Basha R and, Talib R. Antimicrobial Activity of TiO₂ Nanoparticle-Coated Film for Potential Food Packaging Applications. Int J Photoenergy 2014;2014:6. doi:10.1155/2014/945930.
- [87] Long M, Wang J, Zhuang H, Zhang Y, Wu H and, Zhang J. Performance and mechanism of standard nano-TiO₂ (P-25) in photocatalytic disinfection of foodborne microorganisms - Salmonella typhimurium and listeria monocytogenes. Food Control 2014;39:68–74. doi:10.1016/j.foodcont.2013.10.033.
- [88] Altin I and, Sokmen M. Preparation of TiO₂-polystyrene photocatalyst from waste material and its usability for removal of various pollutants. Appl Catal B Environ 2014;144:694–701. doi:10.1016/j.apcatb.2013.06.014.
- [89] Page K, Wilson M and, Parkin I. Antimicrobial surfaces and their potential in reducing the role of the inanimate environment in the incidence of hospital-acquired infections. J Mater Chem 2009;19:3819. doi:10.1039/b818698g.
- [90] Chawengkijwanich C, Hayata Y. Development of TiO₂ powder-coated food packaging film and its ability to inactivate Escherichia coli in vitro and in actual tests. Int J Food Microbiol 2008;123:288–92. doi:10.1016/j.ijfoodmicro.2007.12.017.
- [91] Liu K, Fujishima A, Jiang L and, Cao M. Bio-Inspired Titanium Dioxide Materials with Special Wettability and Their Applications. Chem Rev 2014;114:10044–94. doi:10.1021/cr4006796.

- [92] Higgins C. . multidrug resistance transporters. *Nat Rev* 2007;446:749–55.
doi:10.1038/nature05630.
- [93] Alekshun M and, Levy S. Molecular Mechanisms of Antibacterial Multidrug Resistance. *Cell Mol Neurobiol* 2015;128:1037–50. doi:10.1016/j.cell.2007.03.004.
- [94] Baggot J and, Giguère S. Principles of Antimicrobial Drug Bioavailability and Disposition. *Gen. Princ. Antimicrob. Ther.*, New York: Elsevier Inc.; 2013, p. 41–77.
- [95] Giguère S. General Principles of Antimicrobial Therapy. *Antimicrob. Drug Action Interact.*, New Jersey: Elsevier Inc.; 2013, p. 3–9.
- [96] Lähdetie A, Liitiä T, Tamminen T, Pere J and, Jääskeläinen A. Activation of thermomechanical pulp by laccases as studied by UV-Vis, UV resonance Raman and FTIR spectroscopy. *Holzforschung* 2009;63:745–50. doi:10.1515/HF.2009.125.
- [97] Rohman A, Che Man YB. FTIR spectroscopy combined with chemometrics for analysis of lard in the mixtures with body fats of lamb, cow, and chicken. *Int Food Res J* 2010;17:519–26.
- [98] Agarwal UP, Ralph SA. Determination of ethylenic residues in wood and TMP of spruce by FT-Raman spectroscopy. *Holzforschung* 2008;62:667–75.
doi:10.1515/HF.2008.112.
- [99] Mathew J, Trvisan J, Bassan P and, Rebecca J. Using Fourier transform IR spectroscopy to analyze biological materials. *Nature protocols. J Mater Sci Eng* 2014;9:1771–1791. doi:10.1007/s13398-014-0173-7.2.
- [100] Sanda F, Victor M, Monica T and, Alina C. Spectrophotometric measurements techniques for base theory for UV-Vis spectrophotometric measurements. *Int J Sci Res* 2012;112:45–80.

- [101] Thakkar S, Allegre K, Joshi S, Volkin D and, Middaugh C. An application of ultraviolet spectroscopy to study interactions in proteins solutions at high concentrations. *J Pharm Sci* 2012;101:3051–3061. doi:10.1002/jps.23188.
- [102] Sawant SD. FT-IR Spectroscopy: Principle, Technique and Mathematics. *Int J Pharma Bio Sci Rev* 2011;2:513–9.
- [103] Filip M, Macocian E, Toderas A and, Cărăban A. Base theory for UV-vis spectrophotometric measurements. Hungary-Romania: 2012.
- [104] Vetter W, Englert G, Rigassi N and, Schwieter U. Spectroscopic methods. *Int J Anal Chem* 1971;10:1–124.
- [105] Ohta K, Sadayama S, Togo A, Higashi R, Tanoue R and, Nakamura K ichiro. Beam deceleration for block-face scanning electron microscopy of embedded biological tissue. *Micron* 2012;43:612–20. doi:10.1016/j.micron.2011.11.001.
- [106] Denk W and, Horstmann H. Serial block-face scanning electron microscopy to reconstruct three-dimensional tissue nanostructure. *PLoS Biol* 2004;2:1900–6. doi:10.1371/journal.pbio.0020329.
- [107] Elsukov G, Dorofeev A, Streletski V, Povstugar A and, Protasov E. Determination of nanoparticle sizes by X-ray diffraction. *J Colloid Interface Sci* 2012;74:675–685. doi:10.1134/S1061933X12060051.
- [108] Chauhan A. Powder XRD Technique and its Applications in Science and Technology. *J Anal Bioanal Tech* 2014;5:1–5. doi:10.4172/2155-9872.1000212.
- [109] Banu K and, Cathrine L. General Techniques Involved in Phytochemical Analysis. *Int J Adv Res Chem Sci* 2015;2:25–32.
- [110] Ajayi I, Ajibade O and, Oderinde R. Preliminary Phytochemical Analysis of some

- Plant Seeds. Res J Chem Sci 2011;1:3–7.
- [111] Samatha T, Srinivas P, Shyamsundarachary R, Rajinikanth M and, Rama Swamy N. Phytochemical analysis of seeds, stem bark and root of an endangered medicinal forest tree *Oroxylum indicum* (L) kurz. Int J Pharma Bio Sci 2012;3:1063–75.
- [112] Wadood A, Ghufuran M, Jamal SB, Naeem M, Khan A, Ghaffar R. Analytical Biochemistry Phytochemical Analysis of Medicinal Plants Occurring in Local Area of Mardan. Biochem Anal Biochem 2013;2:2–5. doi:10.4172/2161-1009.1000144.
- [113] Ja T, Sinagawa S., Martínez-ávila G and, López-flores A. *Moringa Oleifera*: phytochemical detection, antioxidants, enzymes and antifungal properties. Int J Exp Bot 2013;9457:193–202.
- [114] Doughari JH. Phytochemicals : Extraction Methods , Basic Structures and Mode of Action as Potential Chemotherapeutic Agents. In: Rao V, editor. Phytochem. A Glob. Perspect. their role Nutr. Heal., Yola, Nigeria: InTech; 2009, p. 1–33.
- [115] Isitua CC, Lozano MJS, Jaramillo C, Farmacia PP De, Ciencias F De, Salud D, et al. Phytochemical and nutritional properties of dried leaf powder of *Moringa oleifera* Lam . from machala el oro province of ecuador. Asian J Plant Sci Res 2015;5:8–16.
- [116] Sahira K and, Cathrine L. General Techniques Involved in Phytochemical Analysis. Int J Adv Res Chem Sci 2015;2:25–32.
- [117] Tekeshwar K, Rizwan A, Kushagra N, Tekeshwar K, Mukesh S and, Dhansay D. Phytochemical estimation of anthraquinones from cassia species. Int J Res Ayurveda Pharm 2011;2:1320–3.
- [118] Islam M, Islam M, Fakhruzzaman M. Isolation and identification of *Escherichia coli* and *Salmonella* from poultry litter and feed. Int J Nat Soc Sci 2014;1:1–7.

- [119] Zahera M, Rastogi C, Singh P, Iram S, Khalid S. Isolation , Identification and Characterization of Escherichia Coli from Urine Samples and their Antibiotic Sensitivity Pattern 2011;1:118–24.
- [120] S Ercis, B Sancak GH. A Comparison of PCR Detection of Meca with Oxacillin Disk Susceptibility Testing in Different Media and Sceptor Automated System for both Staphylococcus aureus and Coagulase-negative Staphylococci Isolates. Indian J Med Microbiol 2008;26:82–100.
- [121] Vineetha N, Vignesh R and, Sridhar D. Preparation , Standardization of Antibiotic Discs and Study of Resistance Pattern for First-Line Antibiotics in Isolates from Clinical Samples. Int J Appl Res 2015;1:624–31.
- [122] Monte J, Abreu A, Borges A, Simões L and, Simões M. Antimicrobial Activity of Selected Phytochemicals against Escherichia coli and Staphylococcus aureus and Their Biofilms. J Pathog 2014;3:473–98. doi:10.3390/pathogens3020473.
- [123] Vipra A, Desai S, Junjappa R and, Roy P. Determining the Minimum Inhibitory Concentration of Bacteriophages : Potential Advantages. Adv Microbiol 2013;2013:181–90. doi:org/10.4236/aim.2013.32028.
- [124] Barbosa HR, Rodrigues MFA, Campos CC, Chaves ME, Nunes I, Juliano Y, et al. Counting of viable cluster-forming and non cluster-forming bacteria: A comparison between the drop and the spread methods. J Microbiol Methods 2007;22:39–50. doi:10.1016/0167-7012(94)00062-C.
- [125] Hayama K, Maruyama N, Abe S. Cell preparation method with trypsin digestion for counting of colony forming units in Candida albicans-infected mucosal tissues. J Med Mycol 2012;50:858–62. doi:10.3109/13693786.2012.683538.

- [126] Brugger SD, Baumberger C, Jost M, Jenni W, Brugger U, Mühlemann K. Automated counting of bacterial colony forming units on agar plates. *PLoS One* 2012;7:1–6. doi:10.1371/journal.pone.0033695.
- [127] Putman M, Burton R, Nahm MH. Simplified method to automatically count bacterial colony forming unit. *J Immunol Methods* 2005;302:99–102. doi:10.1016/j.jim.2005.05.003.
- [128] Musilova L, Ridl J, Polivkova M, Macek T, Uhlik O. Effects of Secondary Plant Metabolites on Microbial Populations : Changes in Community Structure and Metabolic Activity in Contaminated Environments. *Int J Mol Sci* 2016;17:2–31. doi:10.3390/ijms17081205.
- [129] Ganapathi R, Ashok K, Rao V, Chakra S and, Pavani T. Green synthesis of TiO₂ Nanoparticles using Aloe Vera extract. *Int J Adv Res Phys Sci* 2016;2:28–34. doi:2349-7874 (Print) www.arcjournals.org.
- [130] Papaioannou ET, Kapaklis V, Melander E, Hjärvarsson B, Pappas SD, Patoka P, et al. Surface plasmon - Chapter from Rochester. *Opt Express* 2011;19:23867–77. doi:10.1038/nnano.2009.119.
- [131] Almeida M, Erthal R, Padua E, Silveira L and, Am L. Response surface methodology (RSM) as a tool for optimization in analytical chemistry. *J Talanta* 2008;76:965–77. doi:10.1016/j.talanta.2008.05.019.
- [132] Biswas S, Mulaba-bafubiandi AF. Optimization of process variables for the biosynthesis of silver nanoparticles by *Aspergillus wentii* using statistical experimental design. *Adv Nat Sci Nanosci Nanotechnol* 2016;7:11–6. doi:doi:10.1088/2043-6262/7/4/045005.

- [133] Faraway J. Practical Regression and Anova using R. *J Appl Stat* 2002;21:212.
doi:10.1016/0360-1315(91)90006-D.
- [134] Rawlings J, Pantula S and, Dickey D. *Applied Regression Analysis: A Research Tool*.
Second Edi. New York, USA: Springer-Verlag Inc; 1998.
- [135] Dutka M, Ditaranto M, Løvås T. Application of a Central Composite Design for the
Study of NO_x Emission Performance of a Low NO_x Burner. *Energies* 2015;8:3606–
27. doi:10.3390/en8053606.
- [136] Khuri AI, Mukhopadhyay S. Response surface methodology. *Wiley Interdiscip Rev
Comput Stat* 2010;2:128–49. doi:10.1002/wics.73.
- [137] K.B. Tiwari N., Brennan B and C. *Handbook of Plant Food Phytochemicals: Sources,
Stability and Extraction*. Agric. Food Chem., vol. 19, New Jersey: Hoboken: Wiley-
Blackwell; 2006, p. 562–71.
- [138] Fisher L, Ostovapour S, Kelly P, Whitehead K a, Cooke K, Storgårds E, et al.
Molybdenum doped titanium dioxide photocatalytic coatings for use as hygienic
surfaces: the effect of soiling on antimicrobial activity. *Biofouling* 2014;30:911–9.
doi:10.1080/08927014.2014.939959.
- [139] Chen H and, Zhang G. Potent Antibacterial Activities of Ag/TiO₂ Nanocomposite
Powders Synthesized by a One-Pot Sol-Gel Method. *Env Sci Technol* 2009;43:2905–
10.
- [140] Maness PC, Smolinski S, Blake DM, Huang Z, Wolfrum EJ JW. Bactericidal activity
of photocatalytic TiO₂ reaction: Toward an understanding of its killing mechanism.
Appl Environ Microbiol 2008;65:4094–8.
- [141] Brunner T, Grass R and, Stark W. Effect of particle size , crystal phase and

crystallinity on the reactivity of tricalcium phosphate cements for bone reconstruction.

J Mater Chem 2007;17:4072–8. doi:10.1039/b707171j.

- [142] Ruangpan L. Minimal Inhibitory Concentration (MIC) Test and Determination of Antimicrobial Resistant Bacterial. Lab. Man. Stand. methods Antimicrob. Sensit. tests Bact. Isol. from Aquat. Anim. Environ., Tigbauan, Iloilo, Philippines: Southeast Asia Fisheries Development Centre; 2004, p. 31–55.

APPENDIX

Appendix A: Synthesis, characterization and antibacterial studies

List A1: Apparatus

- ❖ Weighing crucible, petri dishes, inoculating loop, 2 mm sieve, beakers, measuring cylinder, conical flask, volumetric flask, test tubes, pestle and mortar, suction filtration apparatus, sterile blades, cuvettes, KBr plate, bolt and nut.

Table A1: Chemical Reagents

| Name | Chemical formula | Manufacturer | Amount |
|--------------------------------|-------------------------------------|---------------------------------------|--------|
| Aqueous Titanium tetrachloride | TiCl ₄ | TOHO Titanium Co Ltd | 1 M |
| Acetic anhydride | (CH ₃ CO) ₂ O | Cosmo chemicals | 40 % |
| Sodium hydroxide | NaOH | Associated chemical enterprises (ACE) | 10 % |
| Iron chloride | FeCl ₃ | Sarchem | 2 % |
| Potassium iodide | KI | Radchem | 99.9 % |
| Chloroform | CHCl ₃ | Sarchem | 35 % |
| Potassium bromide | KBr | ACE | 99.9 % |
| Sulphuric acid | H ₂ SO ₄ | Skylabs | 98 % |
| Distilled water | H ₂ O | MSU Lab | - |
| Muller hinton agar | - | Biochemicals | 500 ml |

Table A2: Instrumentation

| Name | Model | Manufacturer | Use |
|------------------------|--------------|---|--------------------------------------|
| Analytical balance | JJ 224 BC | G&G | Weighing |
| Water bath | ZWY 110X30 | Bibby sterling | Controlling Temperature |
| UV-Vis | UV 752 | Shimadzu | Determination of functional group |
| FT-IR | Nicolet 6700 | Thermo-scientific | Functional group determination |
| Incubator | LABOTEC M15A | Inco-Therm | Optimising E. coli growth |
| Gel Documentational | VISION | SCIE-PLAS | UV Source |
| Autoclave | RAU-123 | SCIE-Masters | Sterilisation |
| Vortex Shaker | QL 866 | WH-2 | Homogenizing |
| Muffle Furnace | SX2-2.5-10 | Zhejiang Sujing Purification Equipment Co., Ltd | Purification, calcining |

Table A3: Effect of pH

| Wavelength (nm) | Absorbance @ pH 5 | Absorbance @ pH 6 | Absorbance @ pH 7 | Absorbance @ pH 8 | Absorbance @ pH 9 |
|--------------------|----------------------|----------------------|----------------------|----------------------|----------------------|
| 200 | 0.34 | 0.33 | 0.35 | 0.33 | 0.30 |
| 300 | 0.23 | 0.25 | 0.30 | 0.28 | 0.25 |
| 400 | 0.56 | 0.61 | 0.75 | 0.73 | 0.66 |
| 500 | 0.44 | 0.46 | 0.55 | 0.50 | 0.45 |
| 600 | 0.25 | 0.30 | 0.34 | 0.25 | 0.31 |
| 700 | 0.20 | 0.22 | 0.26 | 0.20 | 0.20 |

Table A3: Effect of reaction time

| Wavelength Nm | a.u @ 30 min | a.u @ 60 min | a.u @ 90 min | a.u @ 120 min | a.u @ 180 min | a.u @ 240 min | a.u @ 300 min | a.u @ 360 min |
|------------------|-----------------|-----------------|-----------------|------------------|---------------------|---------------------|---------------------|------------------|
| 200 | 0.20 | 0.28 | 0.30 | 0.30 | 0.35 | 0.41 | 0.39 | 0.36 |
| 300 | 0.10 | 0.13 | 0.16 | 0.18 | 0.22 | 0.24 | 0.25 | 0.256 |
| 400 | 0.426 | 0.54 | 0.621 | 0.73 | 0.80 | 0.85 | 0.89 | 0.9 |
| 500 | 0.35 | 0.45 | 0.541 | 0.61 | 0.69 | 0.71 | 0.70 | 0.69 |
| 600 | 0.18 | 0.29 | 0.36 | 0.382 | 0.357 | 0.344 | 0.36 | 0.38 |
| 700 | 0.03 | 0.19 | 0.11 | 0.18 | 0.12 | 0.11 | 0.14 | 0.19 |

Table A4: Method Error Results

| Run | A:TiCl₄ | B:X.Caffra | C:Temperature | Absorbance |
|---------------------------|---------------------------|-------------------|----------------------|-------------------|
| | <i>mM</i> | <i>ml</i> | °C | <i>a.u</i> |
| 1 | 6 | 10 | 25.00 | 0.79 |
| 2 | 6 | 10 | 25.00 | 0.80 |
| 3 | 6 | 10 | 25.00 | 0.78 |
| <i>mean</i> | | | | 0.79 |
| <i>standard deviation</i> | | | | 0.01 |
| $RSD = \frac{100S}{mean}$ | | | | 1.27 % |

Table A5: Colony Forming Unity

| Sample | Condition | E.B.N (loop) | C.F.U | % reduction |
|-----------------------------|--------------|-----------------|-------|-------------|
| TiO ₂ NPs (feed) | UV-radiation | 10 ⁶ | 0 | 100 |
| Distilled H ₂ O | UV-radiation | 10 ⁶ | TNTC | - |

Table A6: Minimum Inhibitory Concentration

| Sample | MIC [mg/ml] |
|-----------------------------|-------------|
| TiO ₂ NPs | 5 |
| TiO ₂ NPs + feed | 11 |

Table A7: Zone of inhibitions (ZOI)

| Concentration (mg/ml) | UV-radiated ZOI | UV-non-radiated ZOI |
|-----------------------|-----------------|---------------------|
| 10 | 6.0 | 1.3 |
| 20 | 6.9 | 2.5 |
| 30 | 7.4 | 3.3 |
| 40 | 8.3 | 3.8 |
| 50 | 9.6 | 4.6 |
| 60 | 11.4 | 5.3 |
| 70 | 12.8 | 5.7 |
| 80 | 14.0 | 6.7 |

Table A8: X. Caffra leaf extract Antibacterial Test

| Disc number | 1 | 2 | 3 | Average |
|--------------------|-----|-----|-----|---------|
| Zone of inhibition | 2.7 | 2.5 | 2.1 | 2.43 |

Table A9: Ashoxy 20TM Oxytetracycline zone of inhibition

| Disc number | 1 | 2 | 3 | Average |
|--------------------|-------|-------|-------|---------|
| Zone of inhibition | 11.50 | 11.42 | 11.67 | 11.53 |

Appendix B: Data treatment

$$\text{❖ Sample Mean} = \bar{x} = \frac{\sum_{i=1}^n x_i}{n} ; \quad \text{Standard deviation, } S = \sqrt{\frac{\sum_{i=1}^n (x_i - \bar{x})^2}{N-1}}$$

○ Where $Y = \text{Sample mean}$

$X = \text{Sample value}$

$n = \text{number of samples}$

$N - 1 = \text{degrees of freedom}$

$$\text{❖ Mean inhibition diameter} = \frac{\text{Summation of inhibition diameters}}{\text{Discs used}}$$

$$\text{❖ } RSD = \frac{100S}{\text{mean}}$$

❖ Preparation of solution concentrations: $C_1V_1 = C_2V_2$: having the initial concentration of aqueous titanium tetrachloride 1M.

Appendix C: Statistical Test

Table C1. Paired T-test of UV- and UV+ at 10 mg/ml

| t-Test: Paired Two Sample for Means | | |
|-------------------------------------|--------------|------------|
| | <i>UV-</i> | <i>UV+</i> |
| Mean | 3.8 | 8.3 |
| Variance | 0.09 | 0.03 |
| Observations | 3 | 3 |
| Pearson Correlation | -0.866025404 | |
| Hypothesized Mean Difference | 0 | |
| Df | 2 | |
| t Stat | -17.00840129 | |
| P(T<=t) one-tail | 0.001719484 | |
| t Critical one-tail | 2.91998558 | |
| P(T<=t) two-tail | 0.003438969 | |
| t Critical two-tail | 4.30265273 | |

From the calculated t-Stat value we can conclude that there is a significant difference in antibacterial activity between the UV-radiated and UV-non-radiated TiO₂ NPs.

Table C2: Paired t-Test of UV+ TiO₂NPs (60mg/ml) and standard drug

t-Test: Paired Two Sample for Means

| | UV+ | Standard |
|------------------------------|--------------|----------|
| Mean | 11.4 | 11.53 |
| Variance | 0.04 | 0.0163 |
| Observation | 3 | 3 |
| Pearson Correlation | 0.31330418 | |
| Hypothesized Mean Difference | 0 | |
| Df | 2 | |
| t Stat | -1.121634752 | |
| P(T<=t) one-tail | 0.189299737 | |
| t Critical one-tail | 2.91998558 | |
| P(T<=t) two-tail | 0.378599474 | |
| t Critical two-tail | 4.30265273 | |

From the calculated t-Stat value we can conclude that there is no significant difference in antibacterial activity of the UV-radiated TiO₂NPs at (60mg/ml) and standard drug.

Table C3: Paired t-Test of UV- TiO₂NPs (60mg/ml) and standard drug

t-Test: Paired Two Sample for Means

| | UV- | Standard |
|------------------------------|--------------|----------|
| Mean | 5.3 | 11.53 |
| Variance | 0.04 | 0.0163 |
| Observations | 3 | 3 |
| Pearson Correlation | -0.979075562 | |
| Hypothesized Mean Difference | 0 | |
| Df | 2 | |
| t Stat | -33.09649793 | |
| P(T<=t) one-tail | 0.000455839 | |
| t Critical one-tail | 2.91998558 | |
| P(T<=t) two-tail | 0.000911678 | |
| t Critical two-tail | 4.30265273 | |

From the calculated t-Stat value we can conclude that there is significant difference in antibacterial activity between the UV-non-radiated TiO₂NPs (60mg/ml) and standard drug.